Environment Agency

Evidence

Measuring landfill methane emissions using unmanned aerial systems: field trial and operational guidance

Report – SC140015

We are the Environment Agency. We protect and improve the environment and make it a better place for people and wildlife.

We operate at the place where environmental change has its greatest impact on people's lives. We reduce the risks to people and properties from flooding; make sure there is enough water for people and wildlife; protect and improve air, land and water quality and apply the environmental standards within which industry can operate.

Acting to reduce climate change and helping people and wildlife adapt to its consequences are at the heart of all that we do.

We cannot do this alone. We work closely with a wide range of partners including government, business, local authorities, other agencies, civil society groups and the communities we serve.

This report is the result of research commissioned and funded by the Environment Agency.

Published by:
Environment Agency, Horizon House, Deanery Road, Bristol, BS1 5AH

www.gov.uk/government/organisations/environment-agency

ISBN: 978-1-84911-367-0

Further copies of this report are available from our publications catalogue:
www.gov.uk/government/publications

or our National Customer Contact Centre:
T: 03708 506506

Email: enquiries@environment-agency.gov.uk

Author(s):
Dr Grant Allen[1]
Mr Joseph Pitt[1]
Dr Peter Hollingsworth[2]
Dr Iq Mead[1]
Mr Khristopher Kabbabe[2]
Mr Gareth Roberts[2]
Prof Carl Percival[1]

[1]Centre for Atmospheric Science
[2]School of Mechanical, Aerospace and Civil Engineering

Dissemination Status:
Publicly available

Keywords:
Unmanned Aircraft System, UAS, Methane, Fugitive emissions, Greenhouse Gases, Landfill, Waste, Spectroscopic Measurement, Remote Sensing

Research Contractor:
Centre for Atmospheric Science, University of Manchester, Oxford Rd, Manchester M13 9PL

Environment Agency's Project Manager:
Mark Bourn, Evidence Directorate

Project Number:
SC140015

Evidence at the Environment Agency

Evidence underpins the work of the Environment Agency. It provides an up-to-date understanding of the world about us, helps us to develop tools and techniques to monitor and manage our environment as efficiently and effectively as possible. It also helps us to understand how the environment is changing and to identify what the future pressures may be.

The work of the Environment Agency's Evidence Directorate is a key ingredient in the partnership between research, guidance and operations that enables the Environment Agency to protect and restore our environment.

This report was produced by the Scientific and Evidence Services team within Evidence. The team focuses on four main areas of activity:

- **Setting the agenda**, by providing the evidence for decisions;
- **Maintaining scientific credibility**, by ensuring that our programmes and projects are fit for purpose and executed according to international standards;
- **Carrying out research**, either by contracting it out to research organisations and consultancies or by doing it ourselves;
- **Delivering information, advice, tools and techniques**, by making appropriate products available.

Miranda Kavanagh

Director of Evidence

Acknowledgements

The authors would like to thank the landfill operator for their support of this project and for access to their landfill sites. In particular, we are thankful for onsite logistical support and for the insight offered into site-specific emissions characterisation and local datasets (long-term wind measurements).

The authors would also like to thank the UK Natural Environment Research Council (NERC) for funding Dr Grant Allen's Fellowship (NE/I021276/1) and the Greenhouse gAs Uk and Global Emissions (GAUGE) project (NE/K00221X/1). These related projects have provided contributions in kind to this project and report, through access to equipment, infrastructure and wider expertise. The authors would also like to thank NERC for funding Joseph Pitt's PhD studentship (NE/L501/591/1) and the University of Manchester for additional funding for the development of UAV platforms through the award of an Engineering & Physical Science Faculty Dean's research-enablement award to develop UAVs for environmental science applications. Finally, we would like to acknowledge Mark Bourn at the Environment Agency for his input, guidance and project management.

Executive summary

This report builds on a previous Environment Agency feasibility study of methane sensing from an unmanned aerial system (UAS), which presented guidance on sensor and platform technology, together with regulatory requirements. Here the aim is to develop and validate a robust method to quantify whole site methane emissions from landfills using measurements from a UAS.

The report describes the development of operational airborne UAS platforms equipped for greenhouse gas sampling with a focus on methane concentration determination along a designated flight path around landfill sites.

The project was conducted in 3 parts:

- development, integration and testing of quasi-static (rotary) and moving (fixed wing) platforms
- planning and execution of a field trial of both systems at a landfill site
- assessment of the data and methane flux methodology with guidance for future operational practice

The platforms were integrated, tested and operated successfully for 10 days of field work, with many important lessons learned for future operational guidance. This report details those activities and provides guidance on flight design and operational practice in varying environmental conditions. It also presents a method for methane flux calculation and uncertainty, and discusses the utility and limitations of the method in practice.

Main findings

These relate to current operational limitations and further work.

There are no current high precision methane instruments (defined in the feasibility study as <40 parts per billion @ 1Hz) suitable for a small fixed wing UAS platform. It is anticipated that such instruments will become available in the near future. Future methane instruments may also be suitable for rotary UAS platforms.

The uncertainty analysis suggests that measurement uncertainty is a very small component of the total uncertainty. This means that it may be possible to yield satisfactory flux uncertainties (<10%) with less precise methane instrumentation than originally suggested. Even less precise instrumentation may be required in cases where the upwind background and the plume morphology can be more adequately constrained and sampled respectively. Instruments with such levels of precision are already becoming available.

The flight control and flight management software stacks for multi-rotors is more mature than the equivalent software for fixed wing UASs. This stems from 2 aspects: the requirement for sophisticated software to control multi-rotors; and the current dominance of photography in the market for small UASs. The result is that, for some applications, multi-rotors are the preferred solution; however, their lower productivity would preclude them from use on larger sites.

The mechanical design limitations also stem from current external market trends. To maximise the productivity of small-fixed wing systems, it is advisable get close to, and remain under, a mass of 7kg. This maximises single flight duration and daily sampling. The issue is that most commercially available, reasonably priced fixed wing systems are not designed to facilitate these operations. Set-up and breakdown time are excessive and individual components are not designed for heavy use. This is in

contrast to similarly sized multi-rotors which often have folding arms and quick release attachments.

The final operational limitation of the mass balance approach is the need to fly circuits of the entire site. This guarantees that both upwind and downwind conditions are sampled, independent of the wind direction, and both lateral extremes of the plume are captured. But due to site access and safety considerations this is not currently possible during normal operational hours. This stems from a combination of site operational procedures and Civil Aviation Authority (CAA) regulations, which require that the aircraft remains 50 metres clear and not overhead of any individuals not under the control of the aircraft operator. This limitation could be addressed by downwind sampling that goes beyond the lateral extent of the plume. This would give a good handle on the background, but may not capture any significant source immediately upwind of the site of interest.

The limitations set out above can easily be addressed through UAS design, construction, careful flight (and sampling) design, and operational procedure development. It is recommended that any production system consists of an integral aircraft, flight control, flight management, sensor system and mission management capability. This allows control over both the hardware and software components, allowing repeatable operations and measurements. Recent changes in CAA policy mean that an operator only has to be cleared to operate a generic <7kg general UAS for aerial work. This reduces the burden of providing an entire system.

Improved software and hardware systems, operator procedures and co-ordination with site personnel have the potential to mitigate the site access limitations. Furthermore, since most operations take place on controlled access sites, it is possible to develop procedures that allow operations across the entire site during normal operational hours.

Emergent methane sensors may be adequate for UAS flux calculation within nominal uncertainties of ~10% in relative terms and are ready to be trialled.

In future work, the approach set out in this report would benefit from further validation against alternative tested approaches to examine sources of systematic bias or uncertainty resulting from sampling.

Contents

List of tables

List of figures

1 Introduction

The aim of this project, which ran for 8 months from September 2014, was to develop and validate a robust method to quantify whole site methane emissions from landfills using measurements recorded from an unmanned aerial system (UAS). This project followed a feasibility study on the use of remote sensing techniques for quantifying methane emissions from landfills (Allen et al. 2014). The feasibility study identified the constraints of power, weight, size, measurement accuracy and sampling methods required to enable field-based statistics of methane flux calculation with a known uncertainty to within ~20%. The conclusion of that study was that suitable and viable measurement platform technologies are achievable within relatively short timeframes (within 12 months). The mass balancing approach was identified as the most promising technique from which to calculate bulk methane fluxes.

The principle behind this project was to test the methane flux measurement techniques discussed in the feasibility study using ‘in situ’ instrumentation (that is, an instantaneous measurement of gas concentration at the place of measurement) and a tailored Lagrangian mass balancing method which requires dense sampling of the emitted plume downwind. The remainder of this report assumes that the reader is broadly familiar with the conclusions of the feasibility study (Allen et al. 2014).[1]

1.1 Structure of this report

Section 2 of this report explains the integration and test of working methane and carbon dioxide UAS measurement platforms. The operation of these platforms in a dedicated field trial is described in Section 3. Section 4 discusses the quality assessment of field trial data. Section 5 examines the flux methodology and principle, and presents the conclusions from the limited trial. Appendix C summarises operational guidance and methods for future methane measurements. A procedure for methane flux calculation, written in the IDL scientific programming language, is provided in Appendix D.

Field measurements from two landfills are used in this report. The two landfills are referred to as Site N and Site O.

[1] The feasibility study report can be downloaded from GOV.UK (https://www.gov.uk/government/publications/aerial-measurements-of-methane-emissions-from-landfills).

2 Platform integration and test

This section describes the building and testing of both a rotary and a fixed wing measurement platform for gas concentration sampling.

As discussed in Allen et al. (2014), there is currently no high precision methane instrument that is suitable to fly on a small fixed wing UAS – though such instruments are in development. Therefore it was elected to develop 2 synergistic platforms for this study:

- a rotary hexrotor platform with a tethered sampling line to sample vertical profiles of methane and carbon dioxide using precision-grade ground instrumentation (Los Gatos ultraportable greenhouse gas analyser – see Allen et al. 2014).
- a fixed wing platform with an onboard precision carbon dioxide infrared reference cell (Edinburgh Instruments Gascard® II, see Section 2.1.2)

The principle behind this approach is that:

- a representative emission ratio (ratio of carbon dioxide to methane) on the day of measurement can be established for any particular landfill using the hexrotor measurements
- methane concentrations in the wider landfill plume can then be inferred by proxy using measurements of carbon dioxide alone on the free-flying fixed wing system

All measurements of carbon dioxide reported here were therefore collected as a proxy for methane in the absence of dedicated UAS methane instrumentation. While landfill emission of carbon dioxide and the nature of its co-emission with methane may be important and interesting in its own right, this study concerns the quantification of methane emissions only. The method described in Section 5 is based on the availability of a suitably precise methane instrument. The details of the dual carbon dioxide and methane approach are discussed further in Section 3. The remainder of this section gives details of the platform and instrumentation.

2.1 Fixed wing carbon dioxide measurement

2.1.1 Platform specifics

An appropriate fixed wing platform identified in Allen et al. (2014) was an aircraft with capabilities similar to the class of the Bormatec Explorer, a twin motor electrically powered aircraft shown in Figure 2.1. Further information is provided in Appendix B. The combination of payload and battery provides sampling durations of approximately 20–30 minutes.

The more open operational regulatory environment and the small size of this type of fixed wing aircraft allows it to be launched and recovered from relatively small, flat grassy spaces, that is, it does not require a road or runway.

The flight trial aircraft, weighing around 5.2kg, was launched using a bungee powered catapult launcher. The catapult allows the system to be launched without using landing gear (saving weight) and without depending on a person to launch the vehicle by throwing it (enhancing safety).

Figure 2.1 Bormatec Explorer aircraft

The fixed wing aircraft has a typical cruise speed of approximately 15 metres per second ($m\ s^{-1}$) or 54 km per hour. This allows it to sample a reasonable area in the available flight time.

For the flight trials, the fixed wing UAS was equipped with:

- a 5-hole probe for three-dimensional (3D) wind profiles
- an Edinburgh Instruments Gascard II carbon dioxide sensor (see Section 2.1.2)
- a PIXHAWK flight control system (FCS) unit, running ArduPlane firmware version 3.2.0
- a dedicated pitot-static probe for estimating airspeed for the FCS unit
- a Beaglebone Black micro-controlling unit running Arch Linux for fusing information from the carbon dioxide sensor, 5-hole probe and FCS unit
- 433 MHz radio telemetry to oversee real-time progress on the mission (via ground station software) and of the sensors (via a terminal window)

A computer running Linux Ubuntu was used as ground station to oversee in real-time the behaviour of the flight control unit and to trigger fail-safe mechanisms in the event of radio control loss.

A wider version of the airframe was used to conduct the flight trials. The wider fuselage allowed the Gascard carbon dioxide sensor to be integrated without further modifications to the airframe. This eased the integration work required to accommodate the sensors at the cost of weight and tighter flight envelope.

The onboard flight control system was tuned to handle the increase in weight. To enhance safety, the aircraft was usually controlled using an envelope protection, self-stabilising mode.

The flight plans shown in Section 3.1.1 were designed taking the capabilities of the system into careful consideration.

2.1.2 Carbon dioxide sensor

The carbon dioxide mole fraction measurements were made onboard the fixed wing UAS using an Edinburgh Sensors Gascard® NG. This utilises non-dispersive infrared (NDIR) sensing technology, where an optical filter is used to select a narrow wavelength band from an infrared light source before it is directed through a gas cell containing the sample. Output intensity from the cell is measured using an infrared detector. The signal generated is a function of the intensity of the light source, the transmittance of the filter, the response of the detector and the absorption due to the sample gas. By analysing the difference between the signal generated at the wavelength of an absorption line of the species of interest and the signal generated at a nearby wavelength separated from the absorption line, instrumental factors can be accounted for and the mole fraction of the target species can be derived.

The model used here has a measurement range of 0 to 2,000 parts per million (ppm) CO_2, sampling at 1 Hz with a measurement uncertainty of ~10 ppm (1σ at 1 Hz). It weighs 0.3kg, making it suitable for use in conjunction with a lightweight battery-powered UAS. Further details on the performance of the Gascard are given in Section 4.2.4.

2.2 Rotary craft methane and carbon dioxide measurement

2.2.1 Platform specifics

The rotary wing platform is a development of work carried out by the University of Manchester on persistent aerial platforms and was custom designed for atmospheric sampling (Figure 2.2). A modified DJI F550 hex rotor aircraft is powered through a tether, which also includes a Teflon sample tube. The tether limits the operational radius of the aircraft but allows for unlimited endurance.

Figure 2.2 Tethered rotary wing aircraft at low altitude

The take-off weight of the aircraft is approximately 600g and it can be operated from any flat surface as long as power is available. It is manually portable and, for the purposes of the trial, was operated from a 2kW petrol generator, which can be refilled while running if necessary.

For trial purposes the altitude was limited to approximately 100 metres by the tether. The aircraft was equipped with:

- an IST AG HYT-271 humidity and temperature sensor
- a Los Gatos Research ultraportable greenhouse gas analyser (LGR-UGGA) on the ground side, attached to the sampling tube
- a PIXHAWK flight control system for position hold
- radio telemetry to oversee real-time progress of the mission via ground station software

A typical field sampling run involved 5 minutes of sampling at 10-metre altitude intervals from 10 to 100 metres.

3 Field trials: operational experience

Field tests were carried out between 20 October 2014 and 20 March 2015 following integration and laboratory testing of the measurement payload described in the previous section.

Flying days were decided based on several parameters including:

- weather and wind direction
- site logistics and site operator permission
- safety and risk considerations

This section describes the typical preparation for flying operation and logistics on the day of data acquisition.

3.1 Preparation for flying operations

Site visits were conducted with site representatives from the landfill operator to jointly decide flying locations, site-specific safety considerations and bases of operations. Following a site visit in October 2014, a plan was developed and discussed with the project management team, including the Environment Agency

3.1.1 Siting and flight considerations

Flight operations must be conducted from a location where permission has been obtained from the landowner to take off and land. In addition, the base of operations should also have good visibility to the horizon and be in an area that can be easily controlled (that is, limited or no public access or where any people present are aware of the activity).

In the case of the field trial at Site N, the landfill operator was also the land owner and permission to work was sought collaboratively after discussion and iteration of prepared risk assessments and method statements. Pre-fieldwork meetings and site visits also allowed the team to choose bases of operations and flight profiles.

A Google Earth image of Site N and nearby built-up areas is shown in Figure 3.1. Flying regulations do not permit overflying of built-up public areas and it was decided not to overfly the active area of the landfill to the south with the fixed wing UAS platform, although flying the static hexrotor was permitted. It was also decided not to overfly the nearby motorway. These choices were made on both scientific and safety grounds; the hexrotor and the precision methane measurements it can sample are required close to the source to derive a characteristic emission ratio (see the example in Figure 5 measured at Site O in August 2014) that represents the landfill source as closely as possible. Proximity to source(s) avoids dilution and contribution of lower concentration extraneous, however the locations of any nearby (non-landfill) sources such as motorways, cattle farms and industry should always be considered when designing sampling programmes to ensure the best possible compromise between proximity to the landfill source and maximum distance from unwanted contaminating sources (see Section 3.2.2).

These safety constraints led to the choice of a base of flying operations for the fixed wing UAS on the north of the site at locations 1 and 2 as marked on Figure 3.1. A further operational site at location 3 was equipped with a 3D sonic anemometer and weather station for continuous measurements between October and the end of November 2014. Field experience meant that this measurement was not strictly required for flux calculation in the flying period in early 2015; wind data recorded by the UAS, together with 2D wind data from a station on the site weighbridge, were suitable for the vertical and reference surface wind speed, respectively.

The purple boxes in Figure 3.1 roughly define pre-programmed (autopilot) flight tracks and waypoints at locations 1 and 2. These flight tracks are an optimised balance of:

- the scientific need to be downwind of source (in specific wind conditions – see Section 4) with some background outside of the plume
- the need to be over permissible and open land
- the need to avoid danger and built up zones

Figure 3.1 Google Earth image of Site N

Notes: The aerial imagery in the figure was recorded on 6 June 2013.

The scale of the image is 2.1 km from left to right extent.

The blue shaded areas show nearby industrial and retail zones, the green shaded area shows the historic (closed) north landfill site and the red shaded area shows the active south landfill site.

A motorway can be seen running north-to-south to the west of the landfill area.

Bases of operations are shown as triangles and numbered numerically.

The purple lines define pre-planned flight tracks for the fixed wing UAS at each location.

3.2 Planning of flying operations

Designated flying weeks were decided on the basis of platform readiness, and pilot and team availability. The project's science lead (Grant Allen) and platform lead (Peter Hollingsworth) would review research-grade weather forecasts for the forthcoming week and identify potential flying days with a 24-hour rolling re-evaluation.

3.2.1 Meteorological conditions: safety

Considerations surrounding weather concern the need for zero (or light, non-frontal) precipitation due to both visibility and site logistics (accessibility) at the time of year. Although the UAS platforms and instrumentation themselves are relatively robust against water, the highly variable winds during frontal or intense shower passage make flight more prone to risk of loss of control. Changing visibility due to rain is also a concern. However, light rain and drizzle can usually be overcome.

Another consideration is the sustained horizontal wind speed and the difference between sustained wind speed and gust speed. The fixed wing UAS chosen for this field trial can fly comfortably at sustained wind speeds of up to 10 m s^{-1}. However, they should not be flown at speeds predicted (or measured on site) to be significantly more than this as sustained wind speeds of greater than 15 m s^{-1} exceed the typical cruise speed of the airframe meaning that the aircraft may not be able to return to base (against such winds), creating a safety risk. In such conditions, the aircraft would be forced to make a controlled safety landing away from the idealised landing location to avoid drifting outside of the pre-designated maximal flying zone. A maximum difference between sustained and gust wind speed was also set to be 10 m s^{-1}.

Sunny days can also be problematic in late autumn, winter and early spring due to the low solar zenith angle, which causes glare for the pilot. While sunny conditions do not preclude flying, they may require re-evaluation of the sampling flight track to avoid glare in the line of sight between pilot location and platform.

3.2.2 Meteorological conditions: science

The conditions considered in Section 3.2.1 together form the meteorological safety criteria for a decision to fly. Further criteria principally concern the wind direction and site logistics, for example, where it was possible and safe to fly and set up a base of operations that permits a flight downwind of the landfill source.

The constraint on bases of operations and land that is permissible to overfly, as described in Section 3.1, meant that the requirement for downwind (and background) sampling limited the range of prevailing wind conditions suitable for flight.

From Figure 3.1, it is clear than a cone of prevailing wind directions between southerly and west to south-westerly would enable full sampling of any plume from the active landfill to the south (not accounting for localised turbulent variability). This cone of wind direction acceptability can be defined for any site by tracing a line from the edge of expected sources to the edges of the available flight track to derive a maximal extent and corresponding wind vector. It is also important to include a portion of the flight track that is outside of the expected plume to derive a background that can be used for differential flux in the Lagrangian mass balancing approach. Figure 4.3 in Section 4.2.1 demonstrates how this can be achieved with knowledge of wind direction and methane concentration.

The constraint described above was perhaps fortuitous as winds in this area at the time of the year chosen for the flying trials are commonly from the west and south-west. However, it further constrained the choice of available flying days in any fixed period. This is an important consideration for future operational work – the more accessible the area around the site of interest, the more versatile the choice of flying day.

With the above in mind, the decision to choose site 1 or 2 as a base was made depending on wind direction on the day. Base 1 was used on days with southerly winds, while Base 2 was used for more south-westerly winds.

Finally, a positive decision to fly was made with a final decision at 24-hours' notice on days when winds were forecast to be both suitable for science and all other meteorological and safety constraints were met as described above. However, this did affect the team's ability to conduct field operations as frequently as they would have liked in the fixed October to March period.

Future work will need to take these considerations into account through careful forward planning tailored to the site of interest and it may be that not all sites lend themselves to this sampling technique. In addition, suitable flying days are likely to be more frequent in the period May to October.

4 Field trial: operations, data and quality assurance

This section demonstrates the data collected during the field trial. Data from a field trial earlier in 2014 at Site O are also presented. Flux calculation and data interpretation are discussed in Section 5.

4.1 Operations

Despite attending Site N a total of 10 times over the period of the project, only 2 successful fixed wing UAS flying operations could be conducted due to onsite logistical problems and platform development challenges. A further 3 hexrotor flights were conducted at Site O in August 2014.

An inability to store equipment at Site N meant that a large volume of equipment had to be loaded and deployed on site on each visit. Furthermore, bases of operations were remote from road access and equipment had to be carried (manually or with the aid of a push trolley) to the required base. This typically required at least 2 hours per day for both set-up and pack-up (4 hours total) and 4 personnel.

The equipment used in the period October to December 2014 is listed below:

- Bormatec Explorer platform, power supplies, ground station and control
- hexrotor platform
- diesel generator (for hexacopter)
- LGR-UGGA
- heavy duty 12V batteries
- 3D sonic anemometer
- 2 metre sturdy tripod – for anemometer
- launch catapult (see Figure 4.1)
- laptop computers
- inlets, tubing and tools

This equipment typically filled a small van and each item of equipment required 2 people for handling.

In November 2014, it was decided to only attempt flights with only one of the 2 platforms on any one day to:

- minimise set-up time and therefore maximise sampling time
- reduce the volume of equipment that had to be carried to the base of operations, which was a significant (15 minute) walk from nearest vehicular access

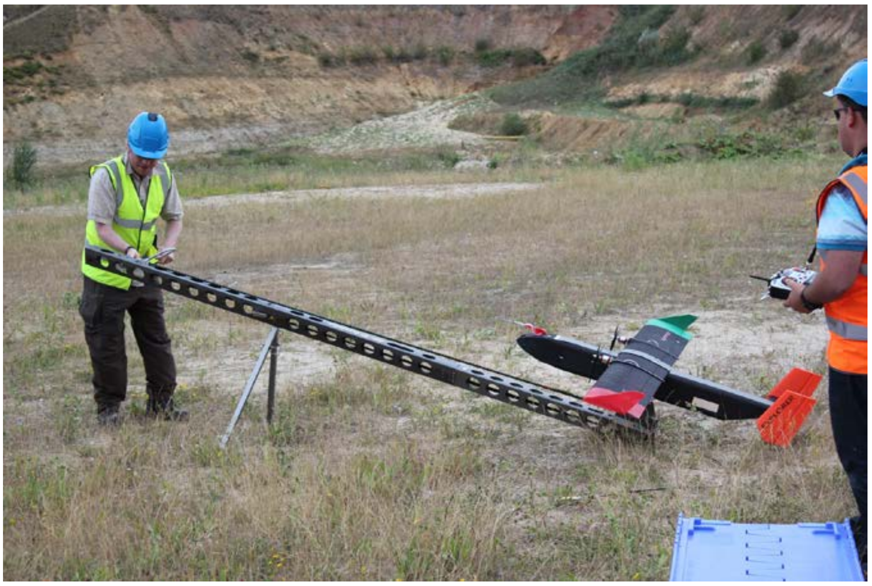

Figure 4.1 The fixed wing UAS take-off catapult

The revised requirement for only one type of flight per day (fixed wing or rotary) meant that the emission ratio defined for one day (by the tethered hexrotor) had to be extrapolated to represent days where only the fixed wing UAS was flown. Repeated hexrotor measurements across several days at Site O suggested that this assumption was reasonable within any one week period (or when source factors may be assumed to be constant, for example, microbial activity, soil temperature profile and moisture content). Ground-based measurements with the LGR-UGGA recorded on the same day as fixed wing UAS flights were also found to yield useful emission ratios without the need to record detailed vertical profiles.

In summary, the fixed wing UAS sampling is the more important measurement (as it captures the spatial extent of the plume) and hexrotor measurements are only important in characterising emission ratios and altitudinal variability for a representative period. Ideally, both platforms would be flown simultaneously and this would be recommended in shorter term operational use. However, this would require rapid set-up and a larger team of people – and 2 pilots. In essence, this describes a compromise between measurement representivity, time constraints and personnel requirements. This is discussed further in Section 5.

4.1.1 Mitigating risk

Well-designed risk assessments, site preparation and planning, and onsite health and safety are all necessary first steps in UAS operations. The flight path design described earlier is an additional part of necessary planning. Implicit in that planning is a ‘plan to fail’, that is, to lose control or crash the UAS platform. Although this risk must clearly be minimised (see below), flying experience to date (across the trained and experienced flying community) indicates that this risk remains non-trivial (that is, a failure of the platform has a probability that requires additional steps to be taken) and it must be assumed that this risk might be realised.

The barriers to realisation of crash risk are many and redundant. As described in Section 2, this includes:

- testing prior to flight on the ground to ensure good pilot-to-platform radio communication
- auto-pilot and telemetry communication to computer ground station

- a trained pilot on standby to take control of the platform who is in line of sight at all times

Pre-programmed way points and exclusion zones (or 'do not cross' boundaries) mean that the auto-pilot will abort the flight using a controlled descent and/or return to base in the event of computed problems or excursions onboard. If that is not possible, control will be handed to the pilot and the pilot can take over at any time in any event. All of the above greatly reduces any risk that the platform could overfly – and therefore potentially crash – into any built-up or other danger area.

In November 2014, an error with the pre-programmed default airframe configuration thresholds programmed for the autopilot software meant that the fixed wing UAS platform flew at an airspeed that was too low to sustain positive lift at high bank angles. After around 10 minutes of normal flight, the fixed wing UAS executed a tight right turn at the eastern waypoint of flight pattern 1 seen in Figure 3.1. Because of the error in nominal airspeed, the platform stalled and executed a dive that the autopilot could then not recover from. At this point, control was handed to the pilot who safely force-landed the platform within the safe zone of the flight path (over the north of the site seen in Figure 3.1). All this demonstrates 2 important points.

- The flight area must always be designed with the assumption that the platform will crash; in that assumption there is mitigation of risk of hazard, damage to property or harm to health.
- In-built redundancy and failure control precautions work effectively.

A robust design of the airframe and payload also meant that expensive equipment was not damaged in the crash and this must also be considered for future platforms. The rebuild and extensive test of the new airframe and auto-pilot system meant that flying operations were postponed between December 2014 and mid-February 2015.

4.2 Field data

Data from a field trial in August 2014 as part of the Natural Environment Research Council's GAUGE project, as well as data from 2 successful flight days on 27 November 2014 and 5 February 2015 are presented here.

4.2.1 Data recorded in August 2014 and rationale for methane proxy method

As discussed in Section 2 and also in Allen et al. (2014), the current absence of a lightweight (less than 5kg), low power, small, precision (defined nominally as >40 parts per billion @ 1Hz) methane instrument (suitable for a small UAS) led to the use in this project of proxy methods – in this case CO_2 concentration – for typical expected landfill methane flux determination.

In summary, this is because CO_2 is co-emitted with methane (CH_4) in landfill gas and existing UAS-suited CO_2 instrumentation can provide sensitivity to detect and resolve small changes in CO_2 concentration relative to background, whereas CH_4 instrumentation capable of resolving small changes relative to background is not yet suited for UAS. However, the method used to derive CO_2 flux here is directly transferrable and analogous to the method and sampling required to derive CH_4 flux using a suitable CH_4 instrument when one becomes available.

Figures 4.2 and 4.3 illustrate the rationale for this proxy approach. Figure 4.2 shows measurements of both CO_2 and CH_4 by the hexrotor system during a trial at Site O in August 2014; fixed wing UAS data were not recorded at Site O. These data were measured by the hexrotor at various heights (as shown on the axis of Figure 4.3) up to 100 metres from the ground using a sampling line to the ground-based LGR-UGGA (see Figure 2.2). Data from 3 separate flights on 2 different days (colour-coded for flight in Figure 4.2) show that CH_4 concentrations scales predictably with instantaneously sampled CO_2 concentration measured downwind of the site. This might be considered to be an optimal case, as this site is close to the sea and therefore distant from other strong local sources that may otherwise perturb the linearity of the relationship seen in Figure 4.2. However, the goodness of fit (or Student's t-test) can yield an uncertainty on this linearity of fit which can be utilised for error propagation when calculating flux by proxy (as discussed in more detail in Section 5).

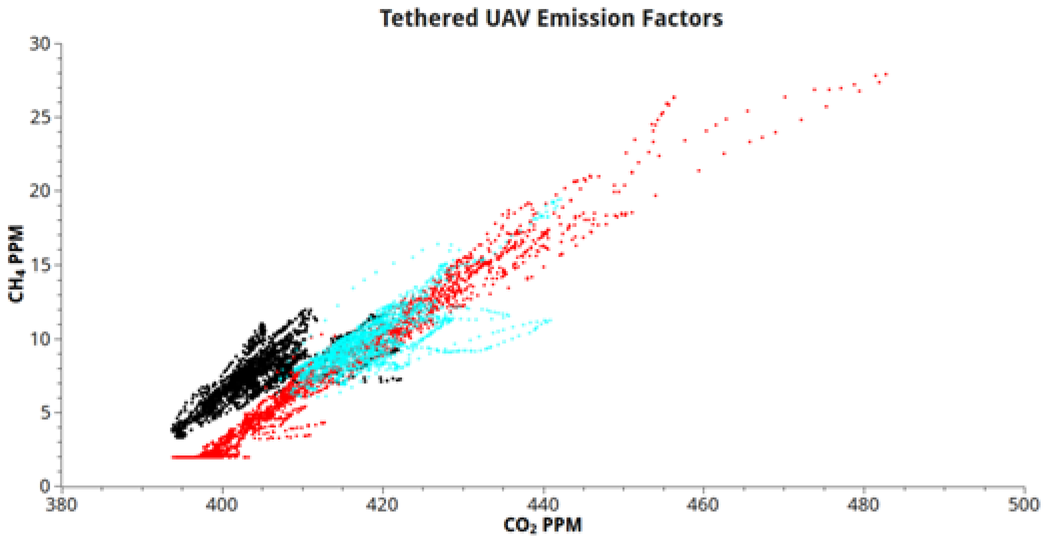

Figure 4.2 Simultaneous carbon dioxide and methane measurements

Notes: The concentration data are shown as dots and were produced using a tethered hexrotor system drawing air down to instrumentation on the ground recorded in August 2014 at Site O and colour-coded for separate flights (black = 5 August 2015, red = 7 August 2015, cyan = 7 August 2015).

Measurements reflect altitudes between ground and 100 metres above sea level (MASL).

A consistent and characteristic emission ratio can be seen.

Knowledge of the wind vector (upwind or downwind of site sources relative to the point of measurement) can also help to give confidence in the linearity of this proxy relationship. Segregating data by wind direction can yield 'landfill influenced' and 'background' variability; the latter is important in accounting for extraneous (offsite) inputs to sampled air downwind or onsite. Figure 4.3 shows this relationship and demonstrates that, for this location, significant enhancements relative to background (red trace in Figure 4.3) were observed only when the wind was coming from the south or the south-east (that is, that the measurement location was downwind of the landfill area).

The sampling inlet on the hexrotor system was positioned more than 20cm above the plane of the rotary blades on the platform. This ensured that air sampled was representative of the height at which it was drawn into the inlet and was not perturbed by the flow of the rotary blades. A 'cone of influence' was defined by computational fluid dynamical modelling for the hexrotor UAS (not shown here) which confirmed that sampling from this distance above the platform ensured no perturbation from the platform itself.

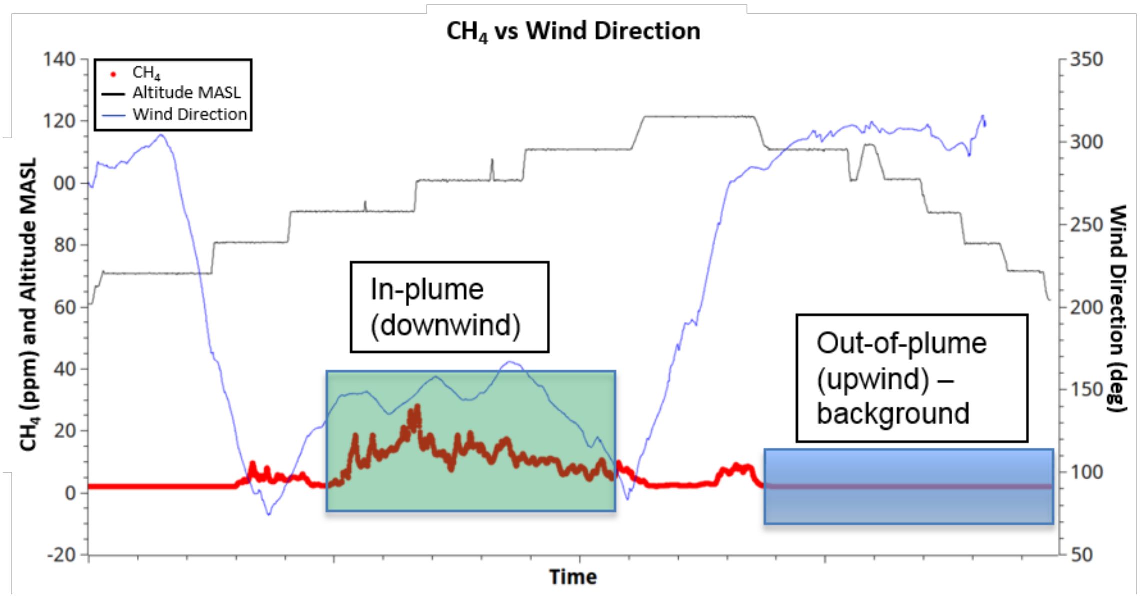

Figure 4.3 Sampled methane concentration in air and its correlation with wind direction from measurements using the tethered hexrotor system in August 2014

In summary, the knowledge that CO_2 and CH_4 are co-emitted from landfill in measureable, predictable and proportional quantities makes it possible to define a scalable parameterisation for CH_4 concentration when the CO_2 concentration is known. Knowledge of wind and background variability also enables the uncertainty when applying this proxy method to be defined. Such a relationship may be assumed to hold true over short periods of time (for example, one day of measurement). However, care would be necessary to ensure such relationships hold over longer timeframes (for example, due to changes in microbial and soil processing associated with changes in environmental parameters).

4.2.2 Data recorded on 27 November 2014

Figure 4.4 shows the flight track of the fixed wing UAS on 27 November 2014. The colour-coded flight track shows areas of low and high CO_2 concentrations measured by the CO_2 Gascard co-located in time and synchronised using the onboard global positioning system (GPS). Lighter (yellow) colours indicate low (more background concentrations) and redder colours represent high concentrations (samples elevated in greenhouse gases).

Higher concentrations can be seen to the west of the flight track. Winds were observed to be light (1–2 m s^{-1}, gusting to 2.5 m s^{-1}), south-westerly and variable on this day. The red lines in Figure 4.4 define an estimate of the edges of the plume corresponding to a wind cone drawn from the edge of exposed landfill along the wind direction. Clearly, on this day, it was not possible to sample the full width of the plume due to the limitations of the flight area. However, the measurements clearly show higher concentrations toward what would conceptually define the centre of any plume advecting from the south site.

Figure 4.4 Flight track and CO_2 concentrations sampled on 27 November 2014

Notes: The blue arrow shows the prevailing wind direction and red lines show the estimated maximal extent of the plume advected from the landfill at the point of sampling.

However, not all enhanced CO_2 measurements represent emission plumes from Site N, especially when outside of the expected cone of plume influence. It was often observed using the LGR-UGGA on the ground that the variable wind direction would deliver air with enhanced concentrations of CO_2, but with more background levels of methane, expected to be due to a mix of both local and regional extraneous sources. The most common of these were enhancements in CO_2 from the west, most likely due to the nearby motorway and from the east due to conurbations and related emissions further afield.

This demonstrates the need for a representative emission ratio for the landfill and good wind direction measurement aloft from which to mask sampled concentrations that do not represent direct emission from the landfill. It is also important to include any error this may introduce into the flux error budget described in Section 5. Most importantly, the derived emission ratio (to which the CO_2 data are scaled) must also use data that represent the source. With this in mind, a threshold of 3 ppm for CH_4 concentration was chosen for the purposes of defining the LGR-UGGA emission ratio – to remove more noisy and emission-diluted air masses from the scaling factor dataset – see Figure 4.9.

The fixed wing UAS Gascard payload and the LGR-UGGA were also operated side-by-side on the ground for 5 minutes before take-off and after landing to provide calibration of the Gascard for CO_2 concentration and to adjust for any small – but typical – systematic offset in the Gascard measurement (see Figure 4.11).

Figures 4.5 and 4.6 show the measurements on 27 November 2014 in more detail. Figure 4.5 shows the data in the horizontal plane as viewed from above. Figure 4.6 shows concentrations in the vertical plane as viewed from the side (to the north in this case). It demonstrates:

- the vertical sampling in this flight including a spiral ascent between ground (which was around 150 m.a.s.l. at the base of operations) and 350 m.a.s.l.
- long-range upward and downward profiles along the east–west track seen in Figure 4.4

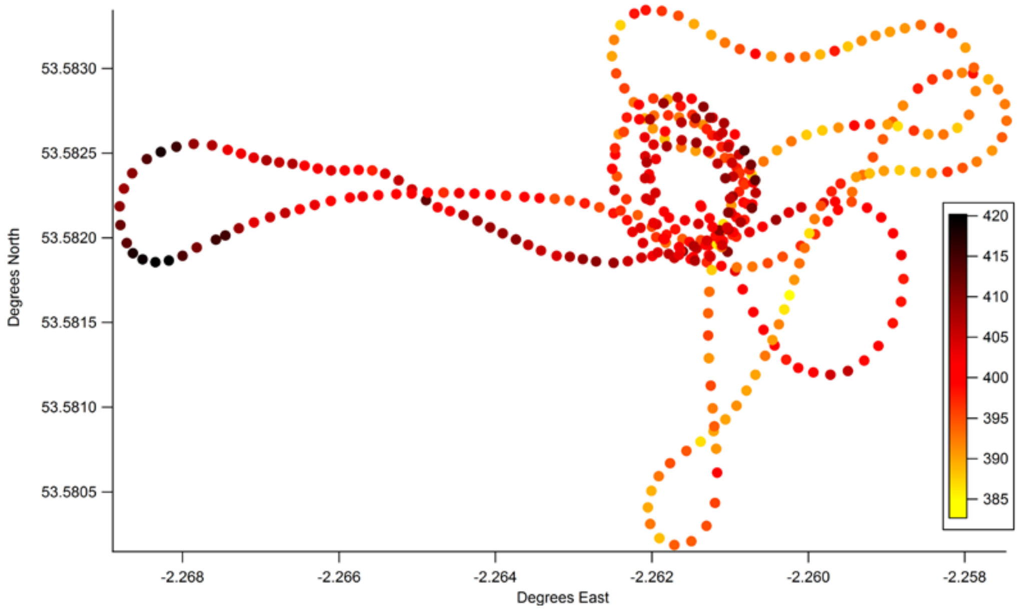

Figure 4.5 Same as for Figure 4.4 but zoomed in and rescaled for clarity of CO_2 concentration enhancements

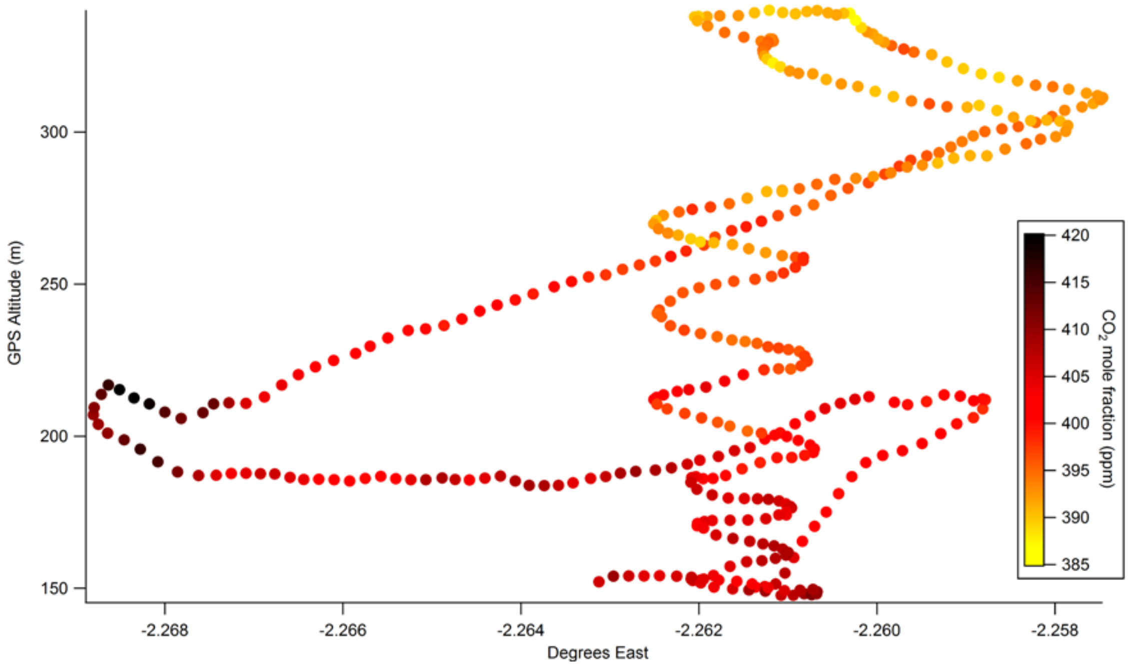

Figure 4.6 Vertically-profiled measurements by the fixed wing UAS as seen from the north of the base of operations (and looking south) scaled for CO_2 concentration

Notes: Altitude is GPS altitude (that is, m.a.s.l).

Ground level was 142 m.a.s.l.

Also seen quite clearly in Figure 4.6 is the gradient in concentration with altitude and with westward extent, which together illustrate the edge and vertical cap of the plume. More dense sampling would more fully map the plume in this case. The westward extent was limited by flight safety and the wind direction meant it was not possible to fully sample the lateral extent of the plume (as described above). However, the extent of the plume and this concentration gradient can be tentatively used to extrapolate the plume beyond the sampling area, albeit with the caveat that this implies an unknown uncertainty that cannot be propagated properly using the mass balancing method.

4.2.3 Data recorded on 5 March 2015

Figure 4.7 shows the flight track viewed from above for 5 March 2015, again colour-scaled to CO_2 concentration. The prevailing wind on this day was south-westerly, relatively strong (3–5 m s^{-1}, gusting 10 m s^{-1}) and less variable than for the previous case.

The consistency of the flight track seen in Figure 4.7 viewed from above is testament to the skill of the auto-pilot in maintaining steady and repeatable sampling patterns. However, Figure 4.8 shows that vertical positioning accuracy is harder to maintain with the fixed wing UAS used here when strong and gusty winds are expected or encountered. The distance end-to-end of this flight track is ~600 metres and each track was performed in around 3 minutes. A total of~15 minutes sampling was achieved. There was no further flying on this day due to strengthening winds which meant that the platform was labouring to stay still (hovering) when flying against the winds aloft. Despite this, the flight was a success and a useful trial of the new field logistical regime and reduced equipment volume described in Section 4.1, which resulted in just an hour to set up and pack up. This would have allowed greater sampling time had the winds not strengthened throughout the day.

The measurements seen in Figures 4.7 and 4.8, which show measurements in the horizontal and vertical plane respectively, show a much more variable concentration pattern than in Figures 4.5 and 4.6 for the 27 November 2014 . This is thought to be because air sampled from a south-westerly direction would be expected to also contain CO_2 emissions from the nearby motorway. This complicates the utility of any emission ratio – see Figure 4.9, which shows ground-based measurements at Site N. It also adds further systematic background error which must be propagated and accounted for using the mass balancing method.

Figure 4.7 Flight track and CO_2 concentrations sampled on 5 March 2015

Notes: Arrows show the prevailing wind direction and red lines show the estimated maximal extent of the plume advected from the landfill at the point of sampling.

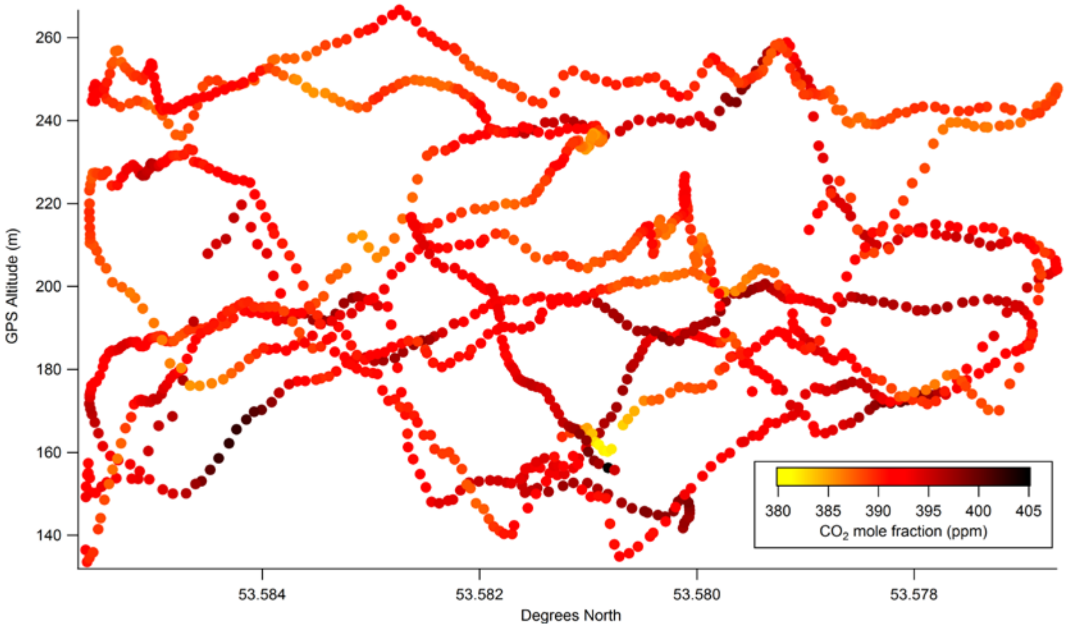

Figure 4.8 Vertically-profiled measurements by the fixed wing UAS as seen from the north (looking south), scaled for CO_2 concentration

Notes: Altitude is measured by GPS (m.a.s.l.).

Figure 4.9 shows a much more variable emission ratio than that seen at Site O in August 2014 (Figure 4.2) or at Site N on 27 November 2014 (Figure 4.10). There is some evidence of a more consistent (straighter) mixing line at higher gradients in Figure 4.9, though it is not possible to disaggregate co-emission of CO_2 and CH_4 from Site N against the variable CO_2 background that is being blown in upwind of site from the motorway.

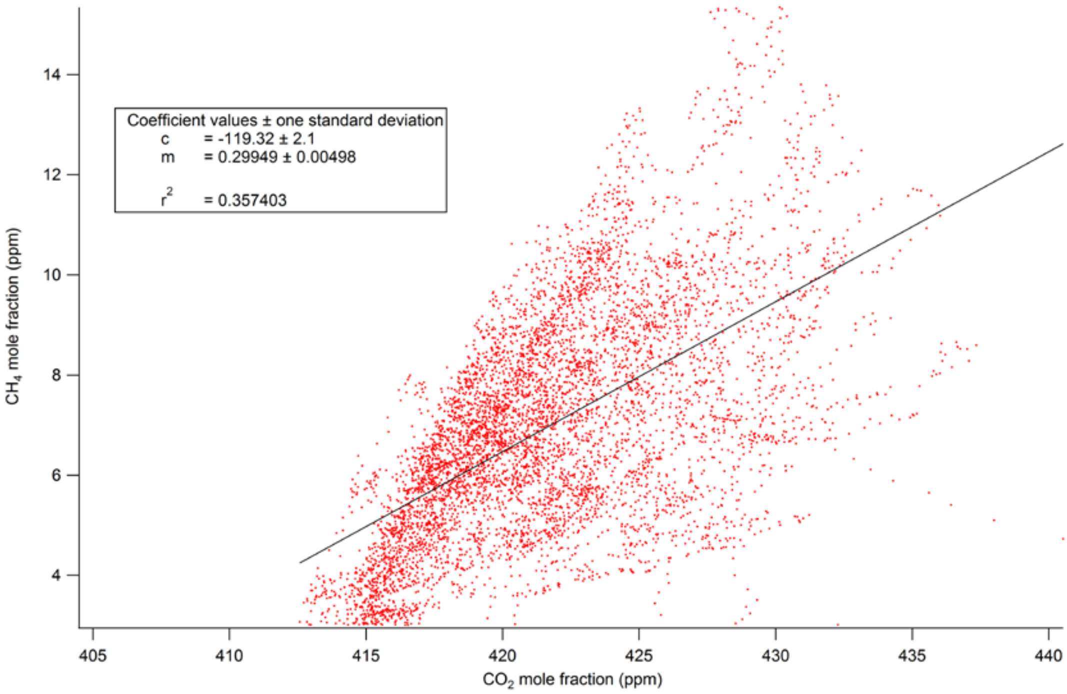

Figure 4.9 Simultaneous carbon dioxide and methane measurements (shown as dots) using LGR-UGGA data recorded on the ground at Base 2 on 5 March 2015

Notes: A fitted line is shown together with fit statistics (correlation).

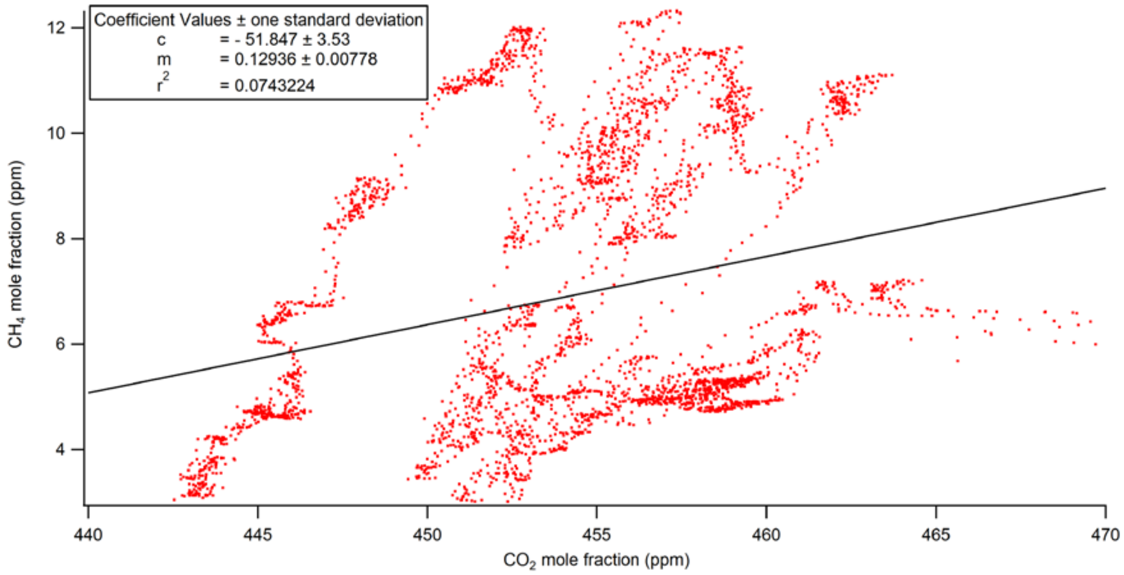

Figure 4.10 Simultaneous carbon dioxide and methane measurements (shown as dots) using LGR-UGGA data recorded on the ground at Base 2 on 27 November 2014

Notes: A fitted line is shown together with fit statistics (correlation).

This is more easily seen in the time series of concentrations of both gases shown in Figure 4.11 on the ground at Base 2. There are clearly periods where CO_2 and CH_4 are well correlated (for example, around 12:02 and 12:07) and it is certain that landfill-influenced air is being sampled. However, there are periods where this is clearly not the case and non landfill-influenced air is sampled – background methane levels are ~2 parts per billion (ppb) but CO_2 is enhanced.

Figure 4.9 illustrates the justification and necessity of choosing the 3 ppm methane threshold from which to use data to calculate an emission ratio. But despite this criterion, the emission ratio remains variable (Figure 4.9) because of the superposition of extraneous and variable CO_2 sources nearby.

Because of the inability to deconvolve these sources in a well-informed way, the most rational method to account for any error this may introduce is therefore to:

1. Calculate an average gradient.
2. Use the variability in the possible range of this gradient to propagate the maximal uncertainty using the mass balance flux equation (see Section 5).

The low r^2 value (0.36) seen in Figure 4.9 suggests that the proxy method is perhaps not well-suited in such wind conditions and for the specific site. Although an uncertainty due to the variability of the background (in this case due to the motorway and other nearby CO_2 sources) can be determined and propagated for the purposes of defining CH_4 flux uncertainty, the uncertainty envelope would be more than 60% (by this one component of the overall error term alone) of the derived flux. This is discussed further in Section 5.

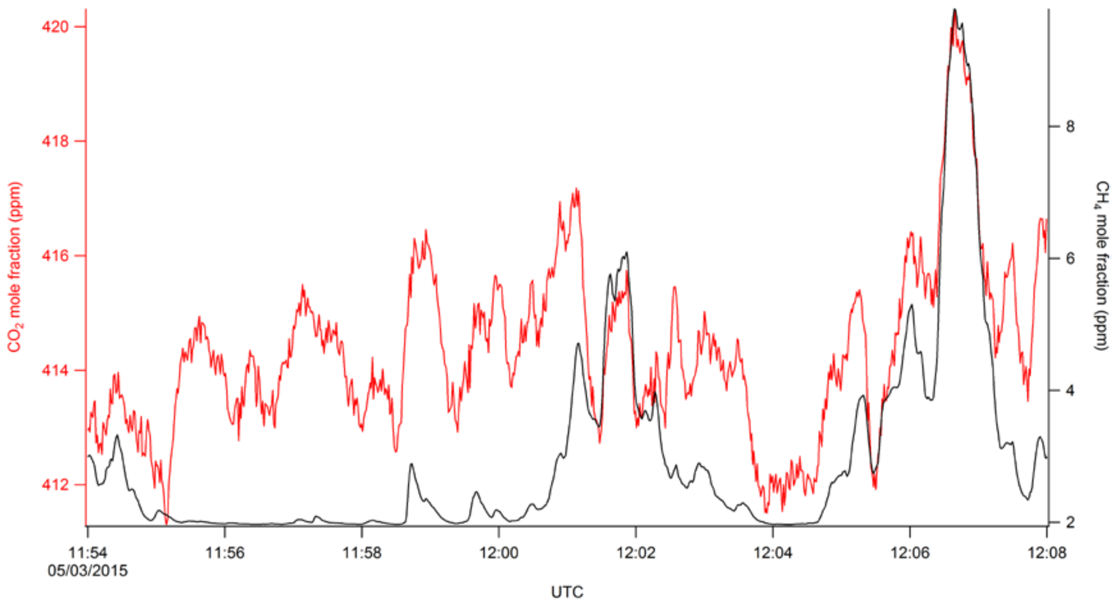

Figure 4.11 Time series of LGR-UGGA carbon dioxide and methane concentration measurements on the ground at Base 2 on 5 March 2015

4.2.4 Laboratory and field calibration

Prior to field deployment, the accuracy and precision of CH_4 measurement using the LGR-UGGA instrument were tested using 2 certified World Metrological Organization traceable gas standards accurate to better than 2 ppb and 0.2 ppm for CH_4 and CO_2 respectively.

The average offset of the LGR-UGGA measured values from the certified cylinder values were −24 ppb CH_4, −0.85 ppm CO_2 for cylinder 1 and −16 ppb CH_4, 0.38 ppm CO_2 for cylinder 2. The 1Hz standard deviations of these measurements were 0.67 ppb, 0.12 ppm, 0.69 ppb and 0.25 ppm respectively. This makes the LGR-UGGA a highly precise instrument in the context of CH_4 and CO_2 enhancements measured in this study. The traceability of the LGR-UGGA calibration makes this a useful calibration instrument for the less precise CO_2 Gascard instrument on the Explorer platform in the field.

Figure 4.12 shows the pre-flight ground-based comparison of the LGR-UGGA CO_2 measurement (red) and the Gascard CO_2 measurement (blue) on 5 March 2015. The 1Hz precision of the Gascard measurements can be seen to be significantly poorer than for the LGR-UGGA; the 1Hz standard deviations for the 2 instruments during this time are 3.51 ppm and 2.20 ppm respectively. There is also a clear systematic negative bias of 10.7 ppm in CO_2 measurements using the Gascard instrument versus the LGR-UGGA. But as the method used (detailed below) relies only on determining the enhancement in CO_2 relative to a background level, all measured using the same Gascard, the absolute value of this offset does not affect the calculated flux, providing that it remains constant with time and is not dependent on CO_2 concentration.

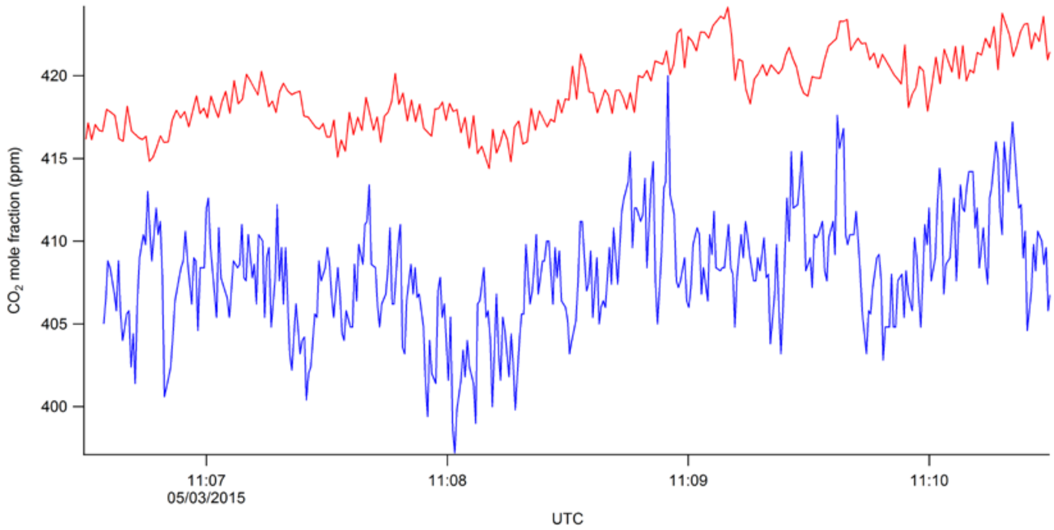

Figure 4.12 Time series of coincident measurements of CO_2 on the ground in the field at Base 2 using the Gascard instrument (blue trace) and the LGR-UGGA (red trace) showing systematic offset used for calibration

Notes: UTC = co-ordinated universal time

4.3 Summary of field trial data

This section summarises the data collected in 3 days of successful field trials of a fixed wing UAS and ground instrumentation at Site N and at Site O.

Concentrations of CO_2 were measured and calibrated using a fixed wing UAS over 2 flights along with wind data and GPS telemetry. Concentrations of CO_2 and CH_4 were also measured simultaneously using data sampled by the LGR-UGGA near to the ground at the base station where the fixed wing UAS was launched (with an inlet positioned 1 metre off the ground) to derive representative emission ratios on both 27 November 2014 and 5 March 2015.

A proxy method was tested to derive CH_4 concentration using linear and scalable relationships using CO_2 concentrations. This was found to be predictable and potentially useful at sites such as Site O, where it can be assumed that there are no significant nearby extraneous (offsite) sources of CH_4 and CO_2 such as those on the coast when winds are blowing from the sea. However, the method was found to be less useful (subject to much higher uncertainty) when practised inland at sites near (within a few km downwind) to sources such as motorways, cities or other strong emitters of either CO_2 or CH_4. Such offsite sources can nullify the requirement that there is a relatively 'flat' or measurable upwind background concentration, resulting in large flux uncertainties when such large background variability is propagated through the flux model.

With this in mind, the proxy method is not always ideal and decisions on siting measurement locations and choosing weather conditions (and hence wind direction) will be important considerations to optimise sampling and to minimise extraneous inputs which may be difficult to account for.

A methane-only measurement fixed wing UAS would have advantages over the system described above due to its ability to bypass the proxy step and any uncertainty that may introduce. However, background variability in CH_4 due to other, potentially different extraneous sources must still be considered when siting measurements and planning sampling. That is, good knowledge of the upwind or out-of-plume environment must still be recorded to assess any variability that must be accounted for in the flux uncertainty.

5 Flux method and conclusions from limited trial

This section describes the method, in principle, for deriving a mass-balanced flux from field data to calculate a nominal flux and flux uncertainty. It should be stressed that this is an illustration of the application of the method in general that should be used with UAS field measurements of methane concentration.

In addition, the flux results from the 2 fixed wing UAS flights are discussed for the Site N field trial only.

5.1 Method and principle

The method for determining a CH_4 flux using mass balancing requires measurements, and spatially geotagged sampling, of methane concentration and horizontal wind velocity from a small fixed wing UAS. This is achieved using the kriged mass balance approach of Mays et al. (2009) described in the preceding feasibility study (Allen et al 2014). Here, CH_4 mole fractions and wind velocities are sampled across a flux plane which is projected downwind of the landfill and interpolated onto a 2D grid, spanning the vertical and horizontal extent of the plume, using a geospatial interpolation technique known as kriging (Myers 1991).

The nature of the racetrack-style sampling seen in Figures 4.8 and 4.9 means that measured data, which are typically at variable distances downwind, need to be projected onto a 2D plane that equates the lateral distance perpendicular to the mean wind vector. This carries the assumption that the plume is not systematically and significantly diluted over the width of the racetrack parallel to the wind, which requires the width of the racetrack to be small relative to the distance downwind. In practice, this requirement will be a compromise between accessible locations to fly downwind and the flying practicalities of the UAS, which requires a finite turning circle.

To better illustrate the method conceptually, an idealised, synthetic dataset of sampled concentrations across a Gaussian plume advected on the wind from a point source is shown in Figure 5.1. In this example, a random but normally distributed error with a 10 ppb standard deviation is added to the pseudo-measured data, which would be consistent with CH_4 measurements using the LGR-UGGA. A UAS ground speed of 15 m s^{-1} is used in this example to re-create a spatial sampling resolution of 15 metres in the horizontal for 4 traverses in the vertical at 50-metre spacing. This example is intended to reflect sparse sampling of an idealised advected plume (subject only to dispersion).

On inspection, a near-surface plume can be seen in the lower centre of Figure 5.1. Assuming a constant (time-invariant) wind field, the measured concentrations in this idealised case would also be unchanging, which would clearly not be expected in real field data (as seen in Section 4). However, this example serves the conceptual understanding of the mass balance approach well.

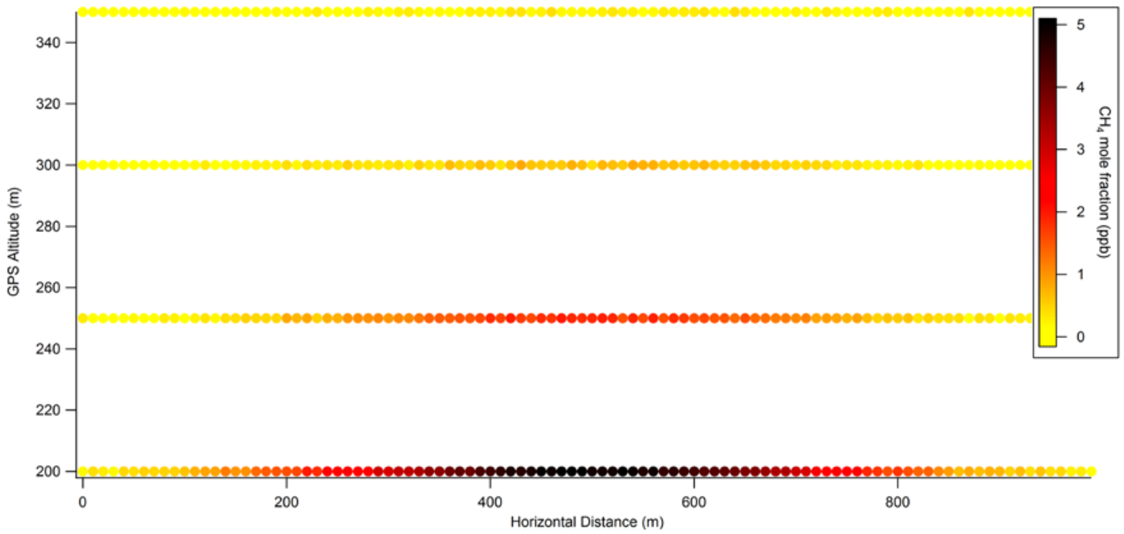

Figure 5.1 Synthetic UAS sampling of a methane plume

Notes: The circles define 1Hz measurements of methane concentration-enhancement-over background along a horizontal flight track across an advecting plume at 4 discrete altitude levels. The colour of each circle defines the sampled concentration as shown in the legend inset.

The next step is to krig the sampled data using a semi-variogram that takes into account:

- the measurement error, that is, how much to 'trust' the measurement at each sample point
- the correlation length, that is, how strongly to weight, with distance, the extrapolated concentration in the null space to its nearest neighbour sample locations
- the limiting variance between pairs of measurements approached as the distance separating them becomes large

In the kriging method, these terms are known as the nugget, range and sill respectively. A full description of the mathematical formalism of kriging is beyond the scope of this report; see Myers (1991) for further information. In summary, the key to successful, and useful, kriging relies on dense and rapid sampling of the plume – a reason why a faster fixed wing UAS is preferred in the near-field to the source.

Figure 5.2 presents the kriged 2D plane of the synthetic data seen in Figure 5.1. This illustration now clearly defines a symmetrical and Gaussian plume that is very well defined at its centre, where enhancement is greatest, and shows less definition at the edges, where the added measurement 'noise' become comparable with the sampled enhancement.

In the example in Figure 5.2, an exponential-type point weighting with a correlation range of 8 times the average distance between points is used – a nugget equal to the 1Hz measurement error of the LGR-UGGA and a sill equal to the full dataset variance. This is appropriate for most UAS applications with good uniform sampling. However, attention should always be paid to define a semi-variogram that best represents knowledge about the system and sampling under investigation as this minimises uncertainty.

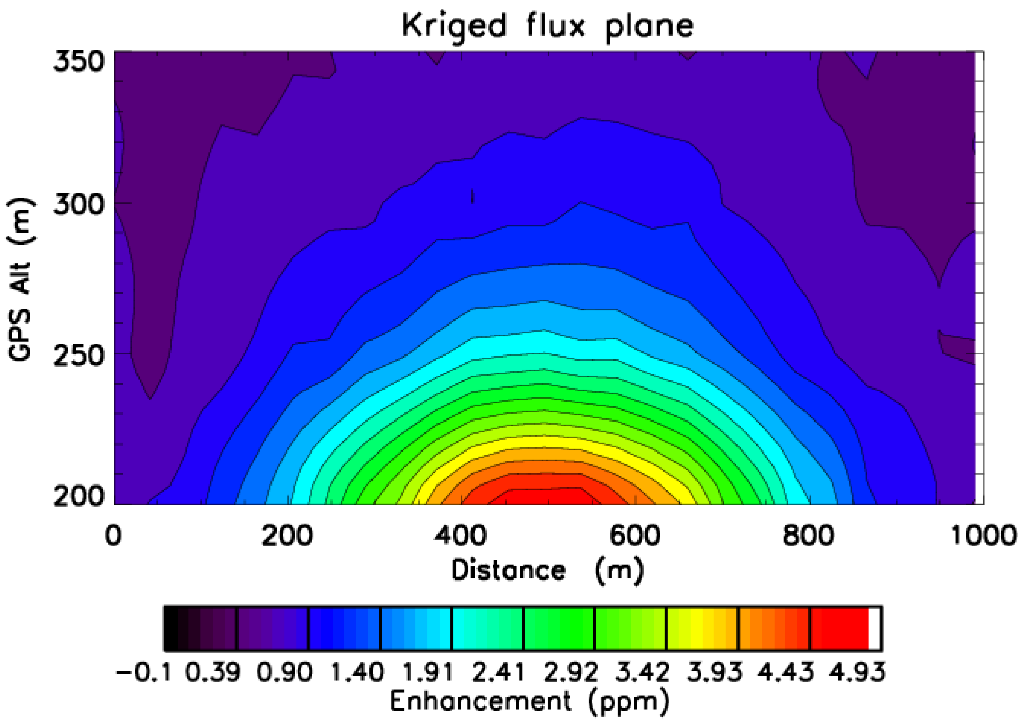

Figure 5.2 Kriged flux plane of methane-enhancement over background using pseudo-sampled data seen in Figure 5.1

Notes: For details of the kriging variogram used in this example, see the discussion in the text.

Having obtained a kriged flux plane downwind (with background subtracted to represent enhancement), a flux is calculated by integrating across the horizontal and vertical extents of the flowing 2D sampling plane which is aligned in the vertical–horizontal plane normal to the prevailing wind:

$$F(CH_4) = \int_o^z \int_A^B (X_{ij} - X_0) n U_{\perp ij} \, dx dz \quad (5.1)$$

where:

X_{ij} is the kriged mole fraction of CH_4

X_0 is the background mole fraction of CH_4 determined by taking an average over the edges of the kriged plane

n is the mole density of air calculated using ground-based measurements of pressure and temperature and assumed constant throughout the plane

$U_{\perp ij}$ is the kriged wind speed perpendicular to the 2D sampling plane, evaluated between ground level and the measured mixing height (*z*), and across and beyond the full width of the plume (*x*) between 2 points A and B.

In the example in Figure 5.2, using a mean wind of 1.5 m s^{-1} and a wind variability/uncertainty of 0.25 m s^{-1}, evaluated across the entire krig flux plane, the methane mass flux in this synthetic example is 0.124 kg s^{-1}. Note that this mass flux is a bulk flux and not a mass flux per unit surface area. However, if the ground surface area of a site of interest is known, then the derived quantity can readily be normalised to the site area to derive an average mass flux per unit surface area.

The same flux equation is used as an error propagation model through which upper and lower bounds on the CH_4 flux can be calculated. This is achieved by measuring or otherwise using knowledge about the uncertainty implicit in each term of the flux equation, that is, concentration measurement precision, sampling bias (kriging uncertainty), vertical mixing height and dilution, and wind variability for example.

Using the uncertainties and natural variability assumed in this illustration, which comprise a 0.25 m s^{-1} (at 1σ) variability in the wind field, a 10 ppb measurement uncertainty (at 1σ), and a 100 ppb background variability (at 1σ), the representative uncertainty on the evaluated flux (also at the 1σ confidence level) is calculated as the sum in quadrature of each error component propagated through the model. This is calculated as 0.023 kg s^{-1} in this example (to 3 decimal places) or ~19% in relative terms.

When using precision, calibrated scientific instrumentation such as that used in this field trial, it is often the variability in the sampled wind field that dominates the uncertainty in the flux calculated using the Lagrangian mass balancing method. In the example above, this wind-related uncertainty comprised ~90% of the total uncertainty on the flux (~0.02 kg s^{-1}), with the background uncertainty comprising 8% and the measurement error accounting for only 2%.

The flux uncertainty arising from the sensitivity to various error components can easily be propagated through Equation 5.1 when designing a sampling system to within a nominal error constraint. In this example, it can be seen that a 100 ppb CH_4 measurement uncertainty would result in only around a 1% uncertainty on the mean flux. Furthermore, if this measurement uncertainty was a Gaussian (random) noise-like error (as opposed to systematic instrumental drift), then this error would scale with the square root of the number of measurements. This is important, as it suggests that in situ instruments with much lower point accuracy (but known noise error profiles) and high sampling rates (for example, 1Hz) can yield meaningful measurements in this context, provided that good repeat sampling is done in the downwind environment.

5.2 Methane fluxes from Site N

Nominal fluxes, and flux uncertainties, are reported here using the limited field trial data for the 2 fixed wing UAS flights discussed in Section 4 and the method described in Section 5.1.

For the flight on 27 November 2014, the mean methane flux was found to be 0.140 kg s^{-1} (to 3 significant figures). The various and total uncertainty components relative to this mean flux are reported in Table 5.1. The table shows that the uncertainty is dominated by the background uncertainty, accounting for 83% of the total flux uncertainty, which is a 59% uncertainty relative to the mean flux itself. There are 2 reasons for this in the case of the field trial data obtained this day.

- The calculation of the background concentration (and background variability) was derived from downwind data (due to siting and flying constraints). It was not possible to confirm that assumed background sampling was not actually partially contaminated by the plume.
- This background was derived from a relatively uncertain emission ratio (Figure 4.10) and the 1σ residual of the emission coefficient has been included in the uncertainty budget for the proxy method used here.

In future, these 2 components can be more tightly constrained by:

- sampling upwind of the site to gain better confidence on the background

- using a precision methane sensor onboard the fixed wing UAS to avoid the convolution of uncertainty that results from the proxy method, where nearby sources of CO_2 may affect the linearity of the emission ratio

Table 5.1 Mean methane flux and 1 standard deviation total (and component) uncertainty for the 2 flight days

	Date of flight	
	27 November 2014	**5 March 2015**
Mean flux	0.14	0.0504
Total uncertainty	0.0854	0.0272
Wind uncertainty	0.0018	0.0051
Background uncertainty	0.0698	0.0139
Measurement uncertainty	0.00289	0.00112
Downwind uncertainty	0.012	0.0071

Notes: All units are in kg s^{-1} and represent the manifestation of error due to spatial sampling and natural sampled variability. See text for discussion.

For the flight on 5 March 2015, the mean methane flux was found to be 0.0504 kg s^{-1}, with a 1σ uncertainty of 0.0261 kg s^{-1}, again dominated by the background uncertainty for the same reasons as discussed for the 27 November 2014 case. The slightly lower relative uncertainty on this day (51% relative to the mean flux) is attributed to the denser downwind sampling compared with 27 November; compare Figures 4.6 and 4.8, which illustrate this).

An interesting conclusion seems to be that the flux on 5 March 2015 was almost 3 times less than on 27 November 2014. This was perhaps because the deeper soil layers were very cold after the winter months, whereas they would still be quite warm from the summer in November, resulting in greater methanogenic activity in November compared with March. However, this is an open question and requires further investigation.

5.2.1 Tracer gas dispersion method

Methane flux was measured using a tracer gas dispersion method at Site N on 21 November 2014.[2] A full description of this flux measurement method, and its relative pros and cons versus the mass balance method discussed in this study, are beyond the scope of this report. However, a comparison of the flux results does give some insight into the potential utility of the 2 methods.

First, the 2 methods are very different and systematic sources of bias common to both methods are not to be expected. The tracer dispersion method uses an inert proxy gas released in known quantities, whereas the mass balancing method measures the plume morphology explicitly. They also measure concentrations of different gases to infer flux so do not suffer from mutual systematic biases associated with background

[2] Under Defra Science and Research Project WR1914, ‘Validation of Alternative Landfill Emissions Testing Methods’.

variability. Therefore, the 2 methods can be assumed to be independent and uncorrelated.

Secondly, the tracer dispersion measurement was conducted on 21 November 2014, while mass balancing fluxes were measured on 27 November 2014 and 5 March 2015. Measurements in November 2014 might be expected to represent a more appropriate comparison, notwithstanding unknown changes in landfill methane flux on the day-to-day timescale.

Finally, all the measurements, analysis and flux calculations by both teams were conducted blind with no knowledge or prediction of the results in advance. Calculated fluxes were only exchanged after they had been calculated independently.

The mean flux measured at Site N by the dispersion method on 21 November 2014 is reported as 523.2 kg $hour^{-1}$ (93.6 kg $hour^{-1}$ at 1σ).[3] This corresponds to 0.148 kg s^{-1} (0.0260 kg s^{-1} at 1σ) in equivalent units to those reported in Table 5.1. Comparison with the 27 November 2014 mass balancing case shows excellent agreement (within 5%) of the mean flux, falling well within the uncertainties calculated for either method.

However, caution is needed in making any conclusion on a validated accuracy for either method based on this one snapshot comparison, especially given that the measurements were not recorded simultaneously. Despite this, this result does lend some additional confidence in both methods within their stated uncertainties. Further simultaneous measurement and blind analysis would be required to build fully validated and quantified assessment of either (or both) method(s).

5.3 Operational guidance and further work

Further guidance on the constraints of UAS sampling and measurement in practice for the application here is provided quantitatively in Appendix C. The issues that lead to this guidance on those constraints are discussed below.

Several basic operational issues were identified and remain after the field trial. These are discussed in turn below.

5.3.1 Availability of methane measurement instruments

As discussed earlier, there are no current high precision methane instruments (defined in the feasibility study as <40 ppb @ 1Hz) suitable for a small fixed wing UAS platform. It is anticipated that such instruments will become available in the near future. Future methane instruments may also be suitable for rotary UAS platforms.

However, suitable instruments for use with a rotary system and a sampling line are currently available. This means that methane concentration and wind data can be obtained from a tethered rotary platform. This could involve vertical sampling (profiling) from a series of locations along a downwind transect. A limitation of this approach could be the longer time taken to sample across the plume as the equipment is moved from one location to the next, but it may be possible to overcome this limitation using portable equipment (for example, in a back-pack). A back-pack for the LGR-UGGA is commercially available. A further advantage of the tethered UAS platform is that size of methane instrument is not a constraint (except for the need to be manoeuvrable on the ground) and high precision methane concentration measurements would be possible.

---

[3] Personal communication by J. Mønster.

In addition, the uncertainty analysis in Section 5.2 suggests that measurement uncertainty is a very small component of the total uncertainty (at ~3% of the total flux in the 27 November 2014 case). This would suggest that it may be possible to yield satisfactory flux uncertainties (<10%) with less precise methane instrumentation than originally suggested. Referring back to the feasibility study (Allen et al. 2014), a measurement precision of ~120 ppb @ 1Hz may then yield flux uncertainties (at least for the measurement component of uncertainty) of less than 10% in relative terms – using the Site O case study as an exemplar.

Even less precise instrumentation may be required in cases (field locations) where the upwind background and the plume morphology can be more adequately constrained and sampled respectively. Instruments with such levels of precision are becoming available. These include:

- the current LI-COR Inc. (USA) Model LI-7700 CH_4 open path commercial-off-the-shelf instrument that might be adapted for UASs
- novel commercial folded path NDIR sensors under development by SenseAir (Sweden)

University groups are known to be investigating these instruments including:

- LI-COR LI-7700 – Dr Rick Thomas, University of Birmingham
- NDIR sensors – Professor Rod Jones, University of Cambridge

The NDIR sensors may offer the greatest potential given their small size (in some cases less than 20 cm × 20 cm) and low power requirements. Current validated precisions for the NDIR instruments are ~100 ppb 1σ @ 1Hz (R. Jones, personal communication, July 2015). The team responsible for the study described in this report will seek to continue to work with these academic colleagues in future trials.

5.3.2 Lack of maturity in fixed wing flight control and management software for small UASs

Flight control and flight management software stacks for multi-rotors is more mature than the equivalent software for fixed wing UASs. This stems from 2 areas:

- the requirement for sophisticated software to control multi-rotors
- the current dominance of photography in the market for small UASs

The result is that, for some applications, multi-rotors are the preferred solution; however, their lower productivity would preclude them from use on larger sites.

5.3.3 Need for improved mechanical design on small, fixed wing UAS systems

The mechanical design limitations also stem from the current external market trends. To maximise the productivity of small fixed wing systems it is advisable get as close to, and remain under, a mass of 7kg. This maximises single flight duration and daily sampling. The issue is that most commercially available, reasonably priced fixed wing systems are not designed to facilitate these operations. Set-up and breakdown time are excessive and individual components are not designed for heavy use. This is in contrast to similarly sized multi-rotors, which often have folding arms and quick release attachments.

5.3.4 Site access constraints prompted by lack of confidence in safe operations and CAA regulations

The final operational limitation is the need to fly circuits of the entire site. This guarantees that both upwind and downwind conditions are sampled, independent of the wind direction, and both lateral extremes of the plume are captured. Currently, because of site access and safety considerations this is not possible during normal operational hours. This stems from a combination of:

- Civil Aviation Authority (CAA) regulations (see Appendix A), which require that the aircraft remains 50 metres clear and not overhead or any individuals not under the control of the aircraft operator
- site operational procedures

A good compromise is to ensure good downwind (but out-of-plume) sampling, that is, to go beyond the lateral extent of the plume. This would also give a good handle on the background but may not capture any significant source immediately upwind of the site of interest (for example, another landfill just behind the site under investigation), though this is unlikely.

In summary, good prior understanding of the site of interest and sampling design are crucial to meaningful results.

5.3.5 Considerations for future trials and operational work

The limitations can easily be addressed through UAS design, construction, careful flight (and sampling) design, and operational procedure development.

It is recommended that any production system consists of an integral aircraft, flight control, flight management, sensor system, and mission management capability. This would consist of both the aircraft and ground station. This allows control over both the hardware and software components, allowing repeatable operations and measurements. This integrated approach does not preclude the use of a modular design that would allow for easier upgrade paths as sensor and computing technology improves. Furthermore, recent changes in the CAA's policy mean that an operator only has to be cleared to operate a generic <7kg general UAS for aerial work. This reduces the burden of providing an entire system.

Improved software and hardware systems, operator procedures and co-ordination with site personnel have the potential to mitigate the site access limitations. Furthermore, since most operations take place on controlled access sites it is possible to develop procedures that allow operations across the entire site during normal operational hours.

Emergent methane sensors such as NDIR may be adequate for UAV flux calculation within nominal uncertainties of ~10% in relative terms and are ripe to be trialled (see Section 5.3.1).

For nominal guidance on quantitative constraints for flux measurement, see Appendix C.

References

ALLEN, G., GALLAGHER, M., HOLLINGSWORTH, P., ILLINGWORTH, S., KABBABE, K., AND PERCIVAL, C., 2014. *Feasibility of aerial measurements of methane emissions from landfills*. SC130034/R. Bristol: Environment Agency.

CAA, 2015. *Air Navigation : The Order and the Regulations*. CAP 393, 4th edition, 10 January 2015. London: Civil Aviation Authority.

MAYS, K. L., SHEPSON, P. B., STIRM, B. H., KARION, A., SWEENEY, C. AND GURNEY, K.R., 2009. Aircraft-based measurements of the carbon footprint of Indianapolis. *Environmental Science & Technology*, 43 (20), 7816-7823.

MYERS, D. E., 1991. Interpolation and estimation with spatially located data. *Chemometrics and Intelligent Laboratory Systems*, 11 (3), 209-228.

Bibliography

CAA, 2015. *SUA: UK National Qualified Entity Approvals and Pilot Competency Requirements*. CAA Information Notice IN-2015/008, 6 March 2015. London: Civil Aviation Authority.

EASA, 2012. *Certification specifications for normal, utility, aerobatic, and commuter category aeroplanes*. CS-23 Amendment 3, 20 July 2012. Cologne, Germany: European Aviation Safety Agency.

EASA, 2013. Certification specifications and acceptable means of compliance for large aeroplanes. CS-25 Amendment 13, 17 June 2013. Cologne, Germany: European Aviation Safety Agency.

List of abbreviations

CAA	Civil Aviation Authority
FCS	flight control system
LGR-UGGA	Los Gatos Research, ultraportable greenhouse gas analyser
m.a.s.l.	metres above sea-level
NDIR	non-dispersive infrared
NERC	Natural Environment Research Council
ppb	parts per billion
ppm	parts per million
UAS	unmanned aerial system

Appendix A: CAA guidelines

The details provided below of applicable articles from Civil Aviation Publication (CAP) Air Navigation Order 393 (CAA 2015) represent an understanding of published CAA guidelines as accessed and reviewed on 16 March 2015.

Table A.1 gives extracts from the Air Navigation Order that are directly or indirectly involve with unmanned aircraft operations.

Table A.1 Relevant extracts from Air Navigation Order 393

Article	Summary
131	Aircraft below maximum take-off weight (MTOW) of 20kg require a 'permission to operate' for commercial work. Said permit is granted by CAA.
137	CAA may require the operator to demonstrate an adequate level of competency as a guarantee that other aircraft will not be endangered. Adequate means of compliance include pilot's licence and Certificate of competency from an approved National Qualified Entity (NQE).
138	CAA may require the operator to demonstrate an adequate level of competency as a guarantee that people, or property are not endangered.
149	Fatigue of crew is required to be addressed in the operations manual
161	CAA has the right to restrict operations at any time.
166	Article specific to small unmanned aircraft (see below) and dictates when an unmanned aircraft can be flown safely.
167	Article specific to UAS equipped with data gathering sensors (see below).
223	CAA has the right to restrict the payload.
224	CAA has the right to approve tariffs.
225	Data gathering operations are restricted for aircraft not registered in the UK.
228	CAA has the right to revoke exemptions.
230	CAA has the right to change terms of permissions given.
232	CAA has the right to ground the aircraft.
256	An aircraft is set to be 'in flight' from the moment it moves by its own accord with the intention of flying.
259	Aerial work is defined as when there is a meaningful consideration exchanged.

Article 166 – Small unmanned aircraft

This article consists of 5 general rules to complement Articles 137 and 138 (see Table A.1), which can be summarised as follows.

(1) A person must not permit any article or animal (whether or not attached to a parachute) to be dropped from a small unmanned aircraft so as to endanger people or property.

(2) The pilot (person in charge of the small unmanned aircraft) must only fly the aircraft if reasonably satisfied the flight can be made safely.

(3) The pilot must maintain visual line of sight (VLOS).

(4) If the aircraft is over 7kg, the aircraft must not be flown:

- in Class A, C, D or E airspace unless permission is granted by air traffic control
- within the vicinity of an airport during the notified hours of watch of air traffic control unless granted by air traffic control, or above 400 feet

(5) Aircraft must not be flown for commercial work, unless permitted by the CAA.

Article 167 – Small unmanned surveillance aircraft

This article consists of 5 rules which apply specifically to aircraft equipped with cameras, data loggers or any other data acquisition system. They can be summarised as follows.

(1) Unless permitted by the CAA, the aircraft must not be flown in any of the circumstances described in paragraph (2).

(2) The circumstances referred to in paragraph (1) are:

(a) within 150 meters of a congested area

(b) within 150 metres of an organised open-air assembly of over 1,000 people

(c) within 50 metres of any vessel, vehicle or structure which is not under the control of the operator of the aircraft

(d) subject to paragraphs (3) and (4), within 50 metres of any person

(3) The aircraft must not be flown within 30 metres of any person during take-off and landing.

(4) Paragraphs 2(d) and (3) do not apply to the operator.

(5) A ‘small unmanned surveillance aircraft’ means a small unmanned aircraft equipped to do surveys, photography or any other form of data acquisition.

Appendix B: Example platform specifications

	CATEGORY	SUB 7KG – FIXED WINGED
	Manufacturer	Bormatec
	Model	Explorer [3]
		
SPECIFICATIONS	Cost	£4000 + sensor
	Powerplant	2 × 550W brushless motor
	Wingspan	220cm
	Take-off and landing	Catapult launch Belly landing
	Payload	2.5kg
	Endurance	>20 metres (2 × 3S 8000mAh @ 15 m s^{-1})
	Avionics	Autopilot for automated waypoint following, take-off and landing
	Suggested payload	Tuneable diode laser spectroscopy (TDLAS) system / Vaisala RS 232 / 5 hole probe

Appendix C: Measurement method

This appendix outlines the aerial methane concentration measurements method to determine a methane flux.

C.1 Limitations of the method

This section sets out the limits to the application of the method for UAS systems with respect to a number of factors.

C.1.1 Wind speed and direction

Wind speed (operational requirement):

- fixed wing UAS platform – prevailing wind must be less than 15 m s^{-1}
- hexrotor platform – prevailing wind must be less than 7 m s^{-1}
- tethered hexrotor platform – prevailing wind must be less than 5 ms^{-1}

Forecast wind direction variability over the sampling period should be to ensure better than 10% flux uncertainty at a nominal wind speed of 5 m s^{-1}, but variable direction as below is advised to be:

- fixed wing UAS platform – less than 20° (at 1σ)
- rotary platform – less than 30° (at 1σ)

C.1.2 Landfill size

The following applies to a landfill site of arbitrary size of 200m × 200m and a wind-speed of 5 m s^{-1}, ignoring all topographic effects and assuming Gaussian dispersion.

For a downwind transect:

- fixed wing UAS platform sampling: 300–1,000 metres downwind, with lateral sampling (width across plume) of 300–500 metres
- hexrotor platform: approximately 100–300 metres
- tethered hexrotor platform: approximately 100–300 metres based on 10-minute vertical flights and sampling locations at 20-metre spacing along the downwind transect (perpendicular to the prevailing wind direction)

For larger landfill dimensions, the sampling location downwind should always be at least 100 metres (preferably up to 300 metres) greater than the landfill width perpendicular to the prevailing wind direction to allow sufficient mixing of the plume. For example, if a landfill were measured to be 500 metres wide (measured perpendicular to the prevailing wind on a given day), the sampling location should be 600–900 metres downwind of the closest edge of the landfill perimeter.

C.1.3 Access requirements

A CAA (or international equivalent) compliant flight path downwind of the landfill should be set; see also Appendix A.

C.1.4 Instrument requirements

A methane sensor meeting the following minimum requirements:

- sampling at 1Hz
- point-precision better than 100 ppb (1σ at 1Hz)
- drift of no more than 100 ppb across period of sampling (single flight) relative to precision calibration before or after flight

A wind sensor meeting the following minimum requirements:

- horizontal wind components (relative to true bearing) better than 0.01 m s^{-1}

A GPS system with the following requirements:

- 3D positional tagging at 1Hz at an accuracy better than 1 metre

C.2 Operational manual and site specific risk assessments

The operational manual is to be agreed with the site operator.

Site-specific risk assessments and method statements are to be produced and agreed.

C.3 Flight path planning

Using the prevailing winds and site specific access details, downwind transect flight paths are defined in compliance with the operations manual and risk assessments.

Where necessary, the flights should be planned for non-operational hours to ensure that the over flown areas are free of people.

Where possible, separate flight paths should be identified to quantify:

- the engine plumes
- separate areas of the landfill (in particular the operational area)

C.4 Data acquisition

Instrument calibration should be conducted and recorded.

The planned downwind transect should be flown when the defined meteorological conditions defined in Section C.1 are met.

Point methane concentrations and wind speed and direction are obtained vertically along the transect.

The extent of the methane plume must be exceeded to determine background methane concentrations.

C.5 Data analysis

The mathematical formalism and method for flux analysis is described in Section 5.1.

We summarize the method here.

The method for determining a CH_4 mass flux using mass balancing requires measurements (and spatially geotagged sampling) of CH_4 concentration and horizontal wind velocity. CH_4 mole fractions and wind velocities are sampled across a flux plane, which is projected downwind of the landfill and interpolated onto a 2D grid, spanning the vertical and horizontal extent of the plume, using a geospatial interpolation technique known as kriging. The nature of the sampling mean that measured data (which are typically at variable distances downwind) must be projected onto a 2D plane that equates the lateral distance perpendicular to the mean wind vector. This carries the assumption that the plume is not systematically and significantly diluted over the width of the racetrack parallel to the wind, which requires the width of the racetrack to be small relative to the distance downwind. In practice, this requirement will be a compromise between accessible locations to fly downwind, and the flying practicalities of the UAS, which requires a finite turning circle (see Section 8.1)

The next step is to krig the sampled data using a semi-variogram that takes into account the measurement error and the correlation length. In the kriging method, these terms are known as the nugget, range, and scale, respectively, and must be determined from the nature of the sampled data. A good starting variogram approximation is recommended as follows: exponential-type point weighting with a correlation range of 8 times the average distance between points, a nugget equal to the 1σ @ 1 Hz measurement error of the methane instrument and a scale of unity. This is appropriate for most UAS applications with good uniform sampling though attention should always be paid to define a semi-variogram that best represents knowledge about the system and sampling under investigation in order to minimize uncertainty and yield the best possible results.

The next step is to use the kriged flux plane downwind (with background subtracted to represent enhancement). A flux is then calculated by integrating across the horizontal and vertical extents of the flowing 2D sampling plane, which is aligned in the vertical-horizontal plane normal to the prevailing wind as follows:

$$F(CH_4) = \int_o^z \int_A^B (X_{ij} - X_0) n U_{\perp ij} \, dx dz$$

where X_{ij} is the kriged mole fraction of CH_4 , X_0 is the background mole fraction of CH_4 determined by taking an average over the edges of the kriged plane, n is the mole density of air calculated using ground-based measurements of pressure and temperature and assumed constant throughout the plane, and $U_{\perp ij}$ is the kriged wind speed perpendicular to the 2D sampling plane, evaluated between ground level and the measured mixing height (z), and across and beyond the full width of the plume (x) between two points A and B.

This same flux equation is used as an error propagation model through which upper and lower bounds on the CH_4 flux can be calculated. This is achieved by measuring or otherwise using knowledge about the uncertainty implicit in each term of the flux equation, i.e. concentration measurement precision, sampling bias (kriging uncertainty), vertical mixing height and dilution, and wind variability for example.

In our experience (when using precision, calibrated scientific instrumentation such as that used in this field trial), it is often the variability in the sampled wind field) that dominates the uncertainty in the flux calculated using the mass balancing method. The flux uncertainty arising from the sensitivity to various error components can easily be propagated through the flux equation when designing a sampling system to within a nominal error constraint.

A procedure written in the IDL scientific programming language is provided in Appendix D for tailoring to specific use. Many of the input parameters are at the user(s) discretion (for example, plume mixing height and width) and must be chosen (ideally) after visual inspection and pre-interpretation of the sampled data and knowledge of the site of interest. A set of defaults are defined in the procedure but it will be important for any operational flux assessment to fully describe the parameters chosen (or used) to allow full transparency and quality assurance of any quantities calculated using the software.

The SC140015 project record IDL 'sav' file and the IDL procedure given in Appendix D can be used to conduct the data analysis (see http://www.exelisvis.com/Support/HelpArticles/TabId/185/ArtMID/800/ArticleID/12395/The-IDL-Virtual-Machine.aspx).

Appendix D: Example algorithm to derive flux from sampling

This Appendix contains text of a commented numerical procedure, coded in the IDL scientific programming language, which can be used to calculate a methane flux from UAS sampled data. It takes pre-formatted, sampled wind, geotag and methane concentration data as inputs to the procedure, krigs these data, and outputs flux and flux uncertainty.

An example test data file is provided as a supplement to this report and the algorithm below can be used with IDL to run the test case example presented in Section 5.1 and seen in Figures 5.1 and 5.2.

```
PRO mass_balance_flux, wind_normal, upsample, downsample, xdist,
ydist, pscale, zcale, meas_err, backgroud=background,
plumez=plumez, plumelateral=plumelateral,$
 test=test, output_status, flux, flux_err, err_msg


set_plot, 'win'
; procedure to calculate mass balanced surface fluxes of trace
gases from 3D upwind and downwind measurements on a krigged flux
plane
; Dr Grant Allen, University of Manchester, May 2015
; grant.allen@manchester.ac.uk

;--------------------------------------------------------------
-
; INPUTS
;----------------------
;
; REQUIRED:
; wind_normal - 1D vector of sampled horizontal wind, calculated
normal to the downwind flux plane (+ ve should be away from
source and vice versa)
; upsample - measured trace gas mass volume concentrations
‘upwind’ of target surface source (units must be kg/kg)
; downsample - measured trace gas mass volume concentrations
‘downwind’ of target surface source (units must be kg/kg)
; pscale - 1D column - density of atmosphere corresponding to
zcale
; zscale - 1D column - GPS altitude scale corresponding to
pscale
; xdist - 1D column - lateral distance (in metres) on the flux
plane from the nominal centre of the plume, that is, distance
from a line normal to the flux plane originating at the centre
of the emission site
; ydist - 1D column - metres above ground level
; meas_err - measurement error in kg/kg
;
; OPTIONAL
;
```

```
; background - keyword - (singular value) - fix assumed
concentration upwind to a singular set value - this will force
the procedure to ignore any upsample input in calculating an
average upwind background
; plumez - keyword - (singular value) - fix the plume height to
a set value - this will force the procedure to define a maximum
mixing height as opposed to defining this from measurement
; plumelateral - keyword - (singular value) - fix the plume
width (diameter) to a set value perpendicular to the plume flux
plane at the point of downwind measurement (that is,
perpendicular to wind).
; test - keyword - if set to 1, the procedure will look for and
use test data sample as an example case
;-------------------------
;
; OUTPUTS
; flux - the mean mass flux per unit time through the downwind
flux plane
; output_status - (1 or 0) - 1 = successful completion, 0 =
error encountered
; flux_err - 1-sigma uncertainty on calculated flux
; err_msg - a string error message if an error was encountered
;-------------------------------------------------------------
-
err_msg='None' ; set initial state
close, /all

; read in test data if test case is specified
IF keyword_set(test) THEN BEGIN
data_file=file_search('c:\flux_data\flux_test_data.txt') ; test
data file must be present in the directory specified here
IF data_file(0) ne -1 THEN BEGIN
backgroundconc=1940. ; ppmv
openr, 1, data_file(0)
dummy=''
line=''
mf=0.
xdist=0.
ydist=0.
readf, 1, dummy ; read in header line
WHILE not eof(1) DO BEGIN
readf, 1, line ; read each data line in turn
test_data=strsplit(line, string(9b), /extract)
mf=[mf,test_Data(2)]
xdist=[xdist,test_Data(0)]
ydist=[ydist,test_Data(1)]
ENDWHILE
; remove unwanted first index data that was needed to read data
in to a dummy array
xdist=xdist(1:*)
ydist=ydist(1:*)
downsample_conc=mf(1:*)*1000.+backgroundconc
; now convert downsample_conc to mass concentration in this test
case -
; note that this should have been pre-calculated for real data
in a
```

```
;higher level procedure that calls this procedure and parses
mass concentrations
downsample=16./28.97*downsample_conc/(1e9) ; convert from ppb to
fractional kg/kg in dry air, noting that molar mass of CH4 is 16
and mean molar mass of dry air is 28.97
background=16./28.97*backgroundconc/(1e9) ; same for background
close, 1
; else set other input variables to arbitrary nominal quantities
for test case
wind_normal=fltarr(n_elements(mf))+1.5+(randomn(seed2, 100,
4)/4.) ; set to mean of 1.5 ms-1 but with some Gaussian
noise/variability , sigma ~0.25 ms-1
plumez=max(ydist)-min(ydist)
plumelateral=max(xdist)-min(ydist)
pscale=1.29 ; assume does not change over height range of UAV
meas_err=6.*16./28.97/1e9
upsample=fltarr(1000)+background+randomn(seed2,
1000)*16./28.97*100./1e9 ; create a background upwind with 100
ppb gaussian variability for test

ENDIF ELSE BEGIN ; if no test data found
print, 'Test data file not found'
output_status=0
err_msg='Test data file not found'
flux=!values.f_nan
fluxsigma=!values.f_nan
return
ENDELSE
ENDIF ; test keyword

; check for a set background or use mean of the upwind sample if
not specified
IF keyword_set(background) THEN downwind_enhance=downsample-
background ELSE downwind_enhance=downsample-mean(upwind)

; krig the data onto a downwind flux plane
; note default number of grid cells for the krigged plane is
25x25 in x and y respectively.
; NOTE: Default krig method is to use exponential point
weighting with a range of 8 times the average distance between
points, a nugget of 0 and scale of 1. This is appropriate for
most UAV applications with
; good (uniform) sampling.
; NOTE2: variogram takes into account the measurement errors at
each sample point and assumes a wide range of 100 x average
point spacing
krigplane=griddata(xdist, ydist, downwind_enhance, /kriging,
variogram=[2, 100, meas_err, 1])

; define axes for a contour plot of the krigged plane
xscale=findgen(25)*(max(xdist)-min(xdist))/24.+min(xdist)
yscale=findgen(25)*(max(ydist)-min(ydist))/24.+min(ydist)
loadct, 39

; convert enhanement on krig plane to units of ppm for plotting
krigplaneppm=krigplane*1e6*28.97/16. ; this assumes methane in
dry air (molar mass of 16 for CH4)
```

```
enhance_scale=indgen(11)*(max(krigplaneppm)-
min(krigplaneppm))/10.+min(krigplaneppm) ; create a nominal 10-
point scale that encompasses the range of data for plotting
purposes later

; plot the kriged flux plane to check enhancement and plume
morphology
set_plot, 'ps'
device, filename='C:\IDL-out\krig_flux_plane.eps', /color,
bits=8 ; check directory exists to accept output plot
contour, krigplaneppm, xscale, yscale, /fill,
nlevels=20,/closed, c_colors=findgen(20)*255./20.,
max_value=max(krigplaneppm), min_value=min(krigplaneppm),$
 background=255, color=0, thick=6, charthick=6, charsize=1.3,
xtitle='Distance (m)', ytitle='GPS Alt (m)', title='Kriged flux
plane',$
 position=[0.1, 0.28, 0.95, 0.9]
contour, krigplaneppm, xscale, yscale, /overplot, nlevels=20,
position=[0.1, 0.28, 0.9, 0.9]
 ; Plot Colourbar.
bar=findgen(600*0.7)
bar=rebin(bar,60, 600*0.7)
tv, bytscl(bar),0.15,0.08, /norm, xsize=0.7, ysize=0.06
FOR i=0, 10 DO BEGIN
xyouts, 0.1+i*((0.7)/10.),
0.04,strmid(strcompress(enhance_scale(i),/remove),0,4),color=0,
/norm, charsize=1.2, charthick=5
plots, [0.15+i*((0.7)/10.), 0.15+i*((0.7)/10.)], [0.14, 0.08],
color=0, /norm, thick=5
ENDFOR
plots, [0.15, 0.15, 0.85, 0.85, 0.15], [0.08, 0.14, 0.14, 0.08,
0.08], color=0, /norm, thick=5
xyouts, 0.37, 0.0, 'Enhancement (ppm)', /norm, color=0,
charthick=5, charsize=1.3
device, /close
set_plot, 'win'

; now run through mass balance flux equation
;;------------------------------
; calculate total volume of air moving through the flux plane
per second
volume=(max(xdist)-min(xdist))*(max(ydist)-
min(ydist))*mean(wind_normal)*mean(pscale) ; units of kg/s

; now calculate flux plane of the trace gas as the enhancement
as a mass fraction of the air mass
fluxplane=krigplane*volume/(n_elements(krigplane)) ; calculate
the mass fluc for each grid cell of the kriged flux plane

; now, finally, integrate the flux over the plane to find the
total flux in the sampled plume
flux=total(fluxplane,/nan) ; kg/s

; now propagate the uncertainties to prescribe a representative
error
upwind_err=stdev(upsample) ; error on background variability
```

```
volume_err=(max(xdist)-min(xdist))*(max(ydist)-
min(ydist))*stdev(wind_normal)*mean(pscale) ; error on advecting
volume due to assumption of homogeneous winds
wind_err_plane=krigplane*volume_err/(n_elements(krigplane))
wind_err=total(wind_err_plane,/nan)

flux_err=sqrt(wind_err^2+upwind_err^2+(meas_err/sqrt(n_elements(
downsample)))^2) ; in kg/s

print, 'Flux: ' + strcompress(flux,/rem)+' kg/s'
print, 'Flux Uncertainty: ' + strcompress(flux_err,/rem)+' kg/s
'+ '(Wind = '+strcompress(wind_err,/rem)+', background =
'+strcompress(upwind_err,/rem)+', measurement =
'+strcompress(meas_err,/rem)+')'
print, ''
print, 'Wind variability: '+strcompress(stdev(wind_normal))+'
m/s'
print, 'Background variability: '+strcompress(stdev(upsample))+'
kg/kg'
print, 'Measurement RMS:
'+strcompress(meas_err/sqrt(n_elements(downsample)))+' kg/kg'

output_status=1
stop
return
END ; pro
```

Would you like to find out more about us or about your environment?

Then call us on
03708 506 506 (Monday to Friday, 8am to 6pm)

email
enquiries@environment-agency.gov.uk

or visit our website
www.gov.uk/environment-agency

incident hotline 0800 807060 (24 hours)
floodline 0345 988 1188 / 0845 988 1188 (24 hours)

Find out about call charges: www.gov.uk/call-charges

Environment first: Are you viewing this on screen? Please consider the environment and only print if absolutely recessary. If you are reading a paper copy, please don't forget to reuse and recycle if possible.